

# Plasma Etching

*An Introduction*

Edited by

**Dennis M. Manos**

*Plasma Physics Laboratory  
Princeton University  
Princeton, New Jersey*

**Daniel L. Flamm**

*AT & T Bell Laboratories  
Murray Hill, New Jersey*



Academic Press  
San Diego New York Boston  
London Sydney Tokyo Toronto

INTEL 1012

This book is printed on acid-free paper. (∞)

Copyright © 1989 by Academic Press

All rights reserved.

No part of this publication may be reproduced or transmitted in any form or by any means, electronic or mechanical, including photocopy, recording, or any information storage and retrieval system, without permission in writing from the publisher.

**ACADEMIC PRESS**

*A Division of Harcourt Brace & Company*

525 B Street, Suite 1900

San Diego, California 92101-4495

*United Kingdom Edition published by*

**ACADEMIC PRESS INC. (LONDON) LTD.**

24-28 Oval Road, London NW1 7DX

**Library of Congress Cataloging-in-Publication Data**

**Plasma etching.**

(Plasma: materials interactions)

Bibliography: p.

Includes index.

1. Plasma etching. I. Manos, Dennis M. II. Flamm, Daniel L. III. Series: Plasma.

TA2020.P5 1988 621.044 87-37419

ISBN 0-12-469370-9

Alkaline paper

PRINTED IN THE UNITED STATES OF AMERICA

97 EB 9 8 7 6

# 3 An Introduction to Plasma Physics for Materials Processing

Samuel A. Cohen  
*Plasma Physics Laboratory  
Princeton University  
Princeton, New Jersey*

|  |     |
|--|-----|
| I. Introduction .....                                    | 186 |
| II. The Plasma State .....                               | 187 |
| III. Single-Particle Motion .....                        | 193 |
| A. $\mathbf{E} = \text{constant}, \mathbf{B} = 0$ .....  | 194 |
| B. $\mathbf{E} = 0, \mathbf{B} = \text{constant}$ .....  | 195 |
| C. $\mathbf{E}$ -perpendicular to $\mathbf{B}$ .....     | 197 |
| D. Non-Uniform Fields and Other Forces .....             | 198 |
| E. Time-Varying Fields .....                             | 201 |
| F. Adiabatic Invariants .....                            | 202 |
| G. Summary of Particle Drifts .....                      | 204 |
| IV. Plasma Parameters .....                              | 205 |
| A. Temperature, Density, and Pressure .....              | 205 |
| B. Debye Length and Plasma Frequency .....               | 207 |
| C. Skin Depth and Dielectric Constant .....              | 213 |
| D. Collisions .....                                      | 217 |
| E. Summary of Plasma Parameters in Practical Units ..... | 229 |
| F. Instabilities .....                                   | 229 |
| G. Plasma Waves .....                                    | 238 |
| V. Discharge Initiation .....                            | 241 |
| A. DC Glow .....   | 241 |
| B. Microwave Breakdown .....                             | 245 |
| VI. An Application—The Planar Magnetron .....            | 248 |
| Acknowledgements .....                                   | 258 |
| References .....   | 258 |

## I. Introduction

The processing of materials by plasmas requires detailed knowledge in several scientific and technological areas. This is particularly true in the field of semiconductor fabrication where the continuing development of denser arrays with finer features has demanded the combination of various techniques into a highly specialized art. Perhaps the basic foundation for this art is plasma physics, though chemistry, electrical engineering, and vacuum technology have defensible claims. Each must be understood and well-practiced for the material processing to succeed.

In this chapter we will present the fundamental concepts in plasma physics which underlie the operation of plasma processing equipment. This will include discussions of the types of particles present in processing plasmas, their energies and fluxes, and an elucidation of the characteristic lengths, time scales, excitable modes (both stable and unstable), and atomic and surface processes important in the initiation and maintenance of plasma discharges. To discuss these topics in a practical way, we include information from a wide range of plasma configurations used in plasma processing, presenting material on dc- and rf-driven discharges with and without externally applied magnetic fields.

The understanding of plasmas that are unmagnetized, isothermal, isobaric, and isotropic is already rather difficult. The configurations used in all processing devices do not have even this simplicity, in large part due to the boundary between the plasma and the solid surfaces. It is at the boundary that our ultimate interests lie. However, the reader should find that the simplified situations described here will form a good understanding of the often counter-intuitive behavior of plasmas and will encourage improvements in existing equipment or processes.

Plasmas are usually created in metal vacuum vessels, commonly used to attain the low pressures essential for particular plasma properties. Plasmas have a propensity to fill every crevice in these vacuum vessels. (The word "plasma" originates from a Greek root meaning deformable.) And though efforts are made to constrain the plasma to particular sections of the vessel, these are not completely successful. Device operation is considerably affected. To emphasize this, we shall use the label "containment" vessels to fully appreciate that some plasma reaches everywhere in them.

We assume familiarity with college physics (especially Maxwell's equations) and introductory calculus. Most equations will be presented both in cgs and practical units to aid their easy application. Section II presents most of the basic ideas and definitions concerning plasmas. These are developed in the later sections. Section III concerns single-particle motion;

Section IV gives details of plasma parameters; Section V is devoted to plasma formation; and Section VI applies the previous four sections to the magnetron device.

## II. The Plasma State

Plasmas are a state of matter that consists of a large group of electrons and ions with nearly equal numbers of opposite charges, each particle moving at a high rate of speed relative to the others. It is the precise electric field of the individual charged particles that gives the plasma its unique properties. The electric field of each particle influences the motion of distant particles, whether they have like or opposite charge. This action-at-a-distance causes a wide variety of waves and instabilities to be possible in a plasma. And because each particle is influenced by the electric and magnetic fields of many particles, the term used to describe the kinematics is *collective motion*.

The electric field of a single isolated electron is proportional to  $r^{-2}$ . The volume of a spherical shell a distance  $r$  from that electron increases proportional to  $r^2$ . Thus, the product of the electric field times the volume, a measure of the effectiveness of the field at a distance, is constant (Fig. 1a). It is the same near the electron as it is far away, showing how the action-at-a-distance arises.

What differentiates a plasma from a group of neutral atoms that also has equal and large numbers of electrons and ions? It is the distance at which the electric field is felt strongly. Neutral atoms (and molecules) have an electric field no stronger than a dipole. This falls-off proportional to the distance cubed or faster. Hence at large distances, it is weak compared to the Coulomb electric field of the bare electrons found in a plasma. Because of the very short range of their electric and magnetic fields, molecules interact with each other only by "hard" collisions, meaning close encounters, typically at separations of about 1 Å. Free electrons and ions in a plasma interact over much greater distances, typically 1000 Å or more, as well as less, of course!

Numerous distant interactions will change a charged particle's trajectory more than the infrequent hard collisions (Fig. 1b). For this reason close encounters may be unimportant to the charged particles in a plasma. (This is related to another reason why a group of neutral atoms does not behave like a plasma. The quantal nature of the electronic energy levels in an atom precludes the small changes in energy required by distant encounters so important to plasma behavior.) Hence plasmas are frequently termed *colli-*

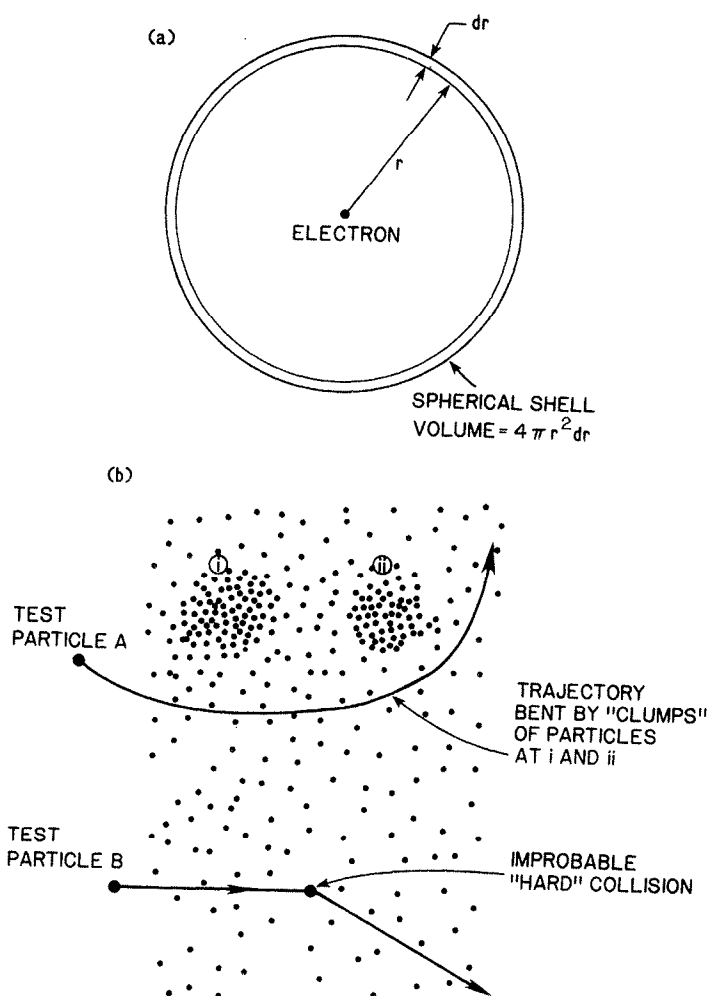


FIGURE 1. a) The electric field of an isolated electron falls off proportional to  $r^{-2}$ . The volume of a spherical shell around that electron increases as  $r^2$ . This shows the importance of distant particles to the motion of that single electron. b) When a charged test particle moves through a cloud of charged particles, the electric field of the distant particles alters the trajectory of the test particle more than the infrequent hard collisions with nearby particles.

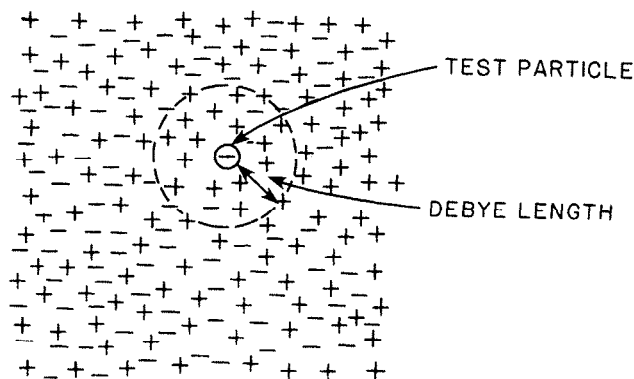


FIGURE 2. When a negative test charge is placed in a plasma, a volume around it, of radius equal to the Debye length, is partially depleted of negative charges. This results in the shielding of that test particle's electric field at distances larger than the Debye length. Outside that volume the negative and positive charges are more nearly equal in abundance.

*sionless*, meaning that individual hard collisions are unimportant compared to the numerous distant soft ones. Exact criteria, which hinge on the characteristic lengths in the problem, must be examined before a particular plasma can be correctly labeled collisionless. For example, is the size of the containment vessel larger than the mean-free-path between hard collisions?

When many charged particles are present, they alter their positions, like-charged particles being repelled and oppositely charged ones being attracted, to reduce the distance over which an applied electric field is effective. The source of this field could be external metal plates attached to a battery, or a single electron placed in the plasma as a *test particle*. The *shielding* (Fig. 2) occurs in a distance called the *Debye length*, whose size determines many properties of the plasma relevant for material processing. The plasmas typically used in materials processing have a Debye length in the range of .01 to 1.0 mm. Within a sphere of this radius there are still many (typically more than a million) charged particles to influence and to be influenced by the test charge.

Shielding does not prevent the penetration of all fields into a plasma. Certain electrostatic and electromagnetic waves, for example, can penetrate into and propagate through plasmas. This is essential to many schemes for plasma heating.

By extrapolation it is clear that, at too high a density, plasma particles may be too close together and thus "appear" like dipoles to the distant particles. Also, at room temperature electrons and ions will rapidly recombine to form neutral atoms and molecules. Hence, to sustain a plasma, its

temperature must be kept above some minimum, about 10,000 K (about 1 eV), which depends on the density. The higher the temperature, the higher is the allowed density. From this, one can estimate that most laboratory plasmas have densities in the range of  $10^8$  to  $10^{12}$   $\text{cm}^{-3}$ .

In astrophysical situations, plasmas exist at much lower densities ( $10^{-3}$   $\text{cm}^{-3}$ ) as in the interstellar medium, and at much higher densities (above  $10^{20}$   $\text{cm}^{-3}$ ) as in certain stars (Fig. 3). Other systems, such as electrons in metals or ions in liquids, also have certain properties like those of our gaseous plasmas.

The approximate equality between oppositely charged particles is termed *quasineutrality*. It is one of the most basic tenets of plasma physics. A 1% excess of either charged species in a plasma with parameters like a magnetron planar etcher would cause an electric field in excess of about 1000 volts/cm. This large field would cause the electrons to rearrange their positions to restore a more balanced distribution of charges. Small electrical imbalances do occur. The resulting restoring force causes the plasma electrons to oscillate internally at a frequency (naturally enough) called the *plasma frequency*. These occur, again for the magnetron etcher, at about  $10^{10}$  Hz.

Three phases of matter—gas, liquid, and solid—are commonly experienced first hand, i.e., they can be readily touched if not too hot or cold. Plasmas cannot. They are generally too hot, too tenuous, and too fragile, almost like a soap bubble. A further similarity to soap bubbles is that the plasma possesses at its boundaries a skin, called the plasma or Debye *sheath*. The sheath is about 5 Debye lengths in thickness. Trying to touch a plasma by penetrating the sheath can destroy the plasma or, if the plasma has enough stored energy, the finger! Hence one of our best ways to test material properties is unavailable. But visual inspection with the naked eye can reveal the presence and dimensions of the sheath, properties of which it has taken scientists decades to confirm and quantify accurately with other diagnostic equipment.

As might be inferred from their densities alone, plasmas behave more like gases than solids. But their modes of internal motion are complex because of collective motion. One similarity is that both support longitudinal compressional (sound) waves. Another is that both expand to fill their containers. On encountering the walls of the containment vessel, the charged particles of a plasma are neutralized by attachment to charged particles from the solid, often metallic, surfaces. Thus, the rate at which the plasma expands will determine how long, and if, it can be sustained. The charged particles lost by contact with the wall must be replaced if the plasma is to continue in its existence (Fig. 4). The steady state thus achieved will depend



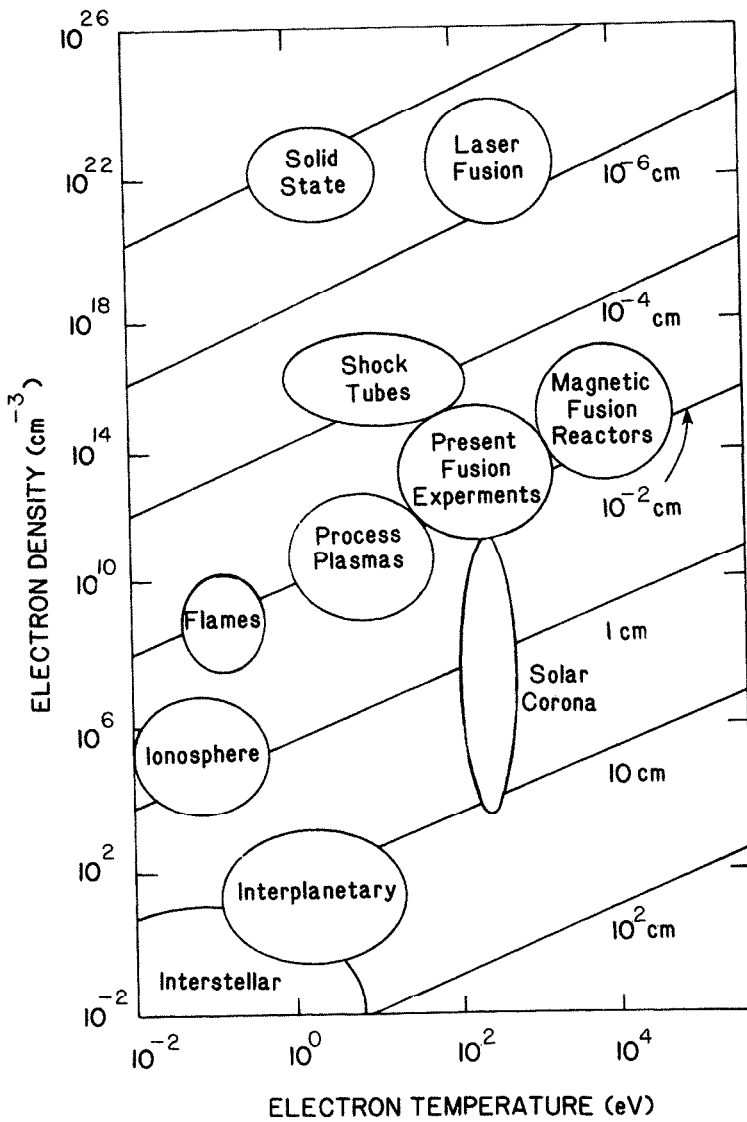


FIGURE 3. Types of plasmas, categorized by their temperatures and densities. The corresponding Debye lengths are the diagonal lines.

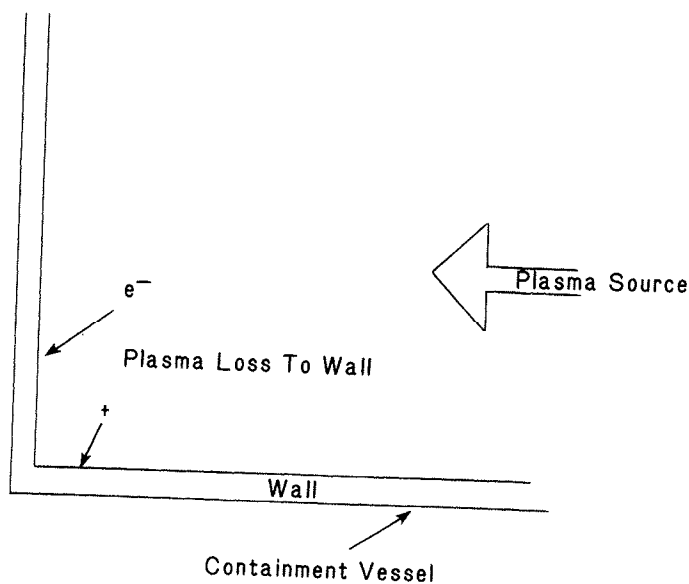


FIGURE 4. Plasma particles are transported to the walls of the containment vessel. There they are absorbed. The lost plasma must be replenished by an internal or external source.

strongly on the properties of the containment vessel, e.g., will it resupply electrons and the right ions when and where needed.

There are numerous ways to replenish the lost particles. Some devices rely on generation of plasma in a separate volume and its injection into the containment vessel. In these apparatus, a plasma "gun" may be used to produce "fresh" plasma by applying a high voltage across a low density gas. Free electrons in the gas are accelerated by the electric field, picking up sufficient energy to ionize any gas atoms they impact. The more usual way to replenish lost plasma is to resupply gas atoms directly into the containment vessel to replace the lost ones and to rely on the impact of the plasma's own electrons to ionize them (Fig. 5). In either case, the ions thus formed may be of several species, depending on the gas feedstock and the plasma parameters. For example, helium gas will form only two types of ions,  $\text{He}^+$  and  $\text{He}^{++}$ , whose abundances will depend on the plasma temperature; in contrast,  $\text{CF}_4$  will be fragmented into nearly a dozen different species. Thus a plasma contains neutral atoms as well as electrons and ions.

Neutral collisions are very important, not just for the chemical processes described in other chapters of this book, but for their effects on plasma behavior. Many properties of the plasma will depend on the relative

Electron Impact Ionization

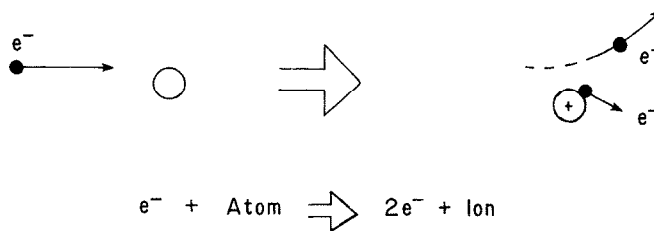


FIGURE 5. The impact of a plasma electron on a neutral atom may result in ionization of that atom.

temperatures and densities of these different species. Though the interaction between the charged particle pairs is much stronger than between a charged particle and a neutral, if the neutral density is very high, then electrons will collide more often with them, and, for example, the electrical resistivity will be affected. The neutral particles in materials processing plasmas typically outnumber the charged ones by more than  $10^4$  to 1. At the extreme, if the neutral to charged particle ratio exceeds about  $10^{11}$ , the neutral collision frequency will exceed the plasma frequency, collective aspects of the motion will be lost, and the plasma state destroyed.

III. Single-Particle Motion

Bulk plasma motion is dominated by collective effects. Yet the motion of each charged particle under the influence of the local electric and magnetic fields is the correct description of what is happening at a microscopic level. And so the Lorentz force law and Maxwell's equations provide the proper way to predict a single test particle's motion. What this approach lacks is the back-effect of the test particle's own motion on the local fields as caused by its fields acting on the distant particles. To improve the single-particle picture, one could start with a description of the plasma as a fluid or as an ensemble of particles. Then fluid equations or the kinetic equations would be used to describe the plasma's evolution. These approaches are usually reserved for the more advanced students. Several references are listed at the end of this chapter that should satisfy the more ambitious. Many results achieved by a kinetic or fluid analysis can be reproduced in a single-particle description by choosing the proper initial conditions based on the known answer. This is often done for pedagogical reasons because the single particle picture is so easy to visualize and hence to remember. We use this

approach here.

In the single-particle approach to plasma physics, the motion of an individual charged particle under the influence of externally applied electric and magnetic fields is examined. The fields are allowed to vary in space and time but do not change to reflect the subsequent motion of the charged particle. The motion of the single particle is readily obtained from the Lorentz force law, which (in cgs units) is

$$\mathbf{F} = \frac{m d\mathbf{v}}{dt} = q\left(\mathbf{E} + \frac{\mathbf{v} \times \mathbf{B}}{c}\right), \quad (1)$$

where  $c$  is the speed of light ( $3 \times 10^{10}$  cm/s),  $m$  is the mass of the charged particle (in gm),  $q$  its charge ( $-4.8 \times 10^{-10}$  statcoul for a single electron),  $v$  its velocity (cm/s), and  $E$  (in statv/cm) and  $B$  (in gauss) are the applied electric and magnetic fields, respectively. We now discuss several simple cases of this equation.

#### A. $\mathbf{E} = \text{CONSTANT}$ , $\mathbf{B} = 0$

The application of a constant and homogeneous electric field, but no magnetic field, results in the constant acceleration of a charged particle. The particle gains energy from the field at an ever increasing rate. If allowed to continue, the particle would eventually reach relativistic speeds. Then the simple Newtonian description fails and the particle gains mass rather than speed, and also energy and momentum. This relativistic limit is beyond the scope of processing plasma physics. Integrating Eqn. (1) for  $E$  parallel to the  $x$ -direction gives

$$x(t) = x_0 + v_{x0}t + \frac{qEt^2}{2m}, \quad (2)$$

where  $x_0$  and  $v_{x0}$  are the initial  $x$ -position and  $x$ -velocity of the particle. If the initial velocity  $v_0$  is zero or is in the direction parallel to  $E$ , this motion is in a straight line. Otherwise it is parabolic (Fig. 6). Though in most

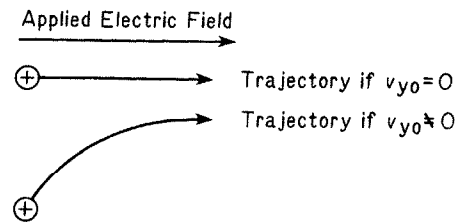


FIGURE 6. Trajectories of charged particles in a constant electric field.

situations it is adequate to ignore a particle's past history, i.e.,  $x_0$  and  $v_0$ , this is not true in the initiation of a discharge or in most microwave-driven discharges.

B.  $E = 0, B = \text{CONSTANT}$

As seen from the Lorentz law, if there is no electric field and no initial velocity, the particle remains at rest. More precisely, the magnetic force acts only if the particle's motion is perpendicular to  $B$ . The result is that a particle moving initially along  $B$  is unaffected by  $B$  while a particle moving perpendicular to  $B$  has its trajectory turned into a circle. For a particle moving at an angle to  $B$  the net result is a corkscrew or helical motion. There is no gain or loss of total particle kinetic energy from a static or slowly varying magnetic field (Fig. 7). Integrating Eqn. (1) for this choice of parameters gives

$$\begin{aligned} z(t) &= z_0 + v_{z0}t \\ x(t) &= x_0 + r_L \sin(qBt/mc) \\ y(t) &= y_0 + r_L \cos(qBt/mc) \end{aligned} \tag{3}$$

where

$$r_L = \frac{mv_{\perp}c}{qB}, \tag{4}$$

$v_{\perp}$  is the component of the velocity perpendicular to  $B$ , and we assumed  $B$  parallel to  $z$ ,  $B = B_z$ .

Notice that the circular motion has a characteristic radius,  $r_L$ , called the *Larmor radius*, and a characteristic frequency,  $\omega_c = 2\pi f = qB/mc$ , called

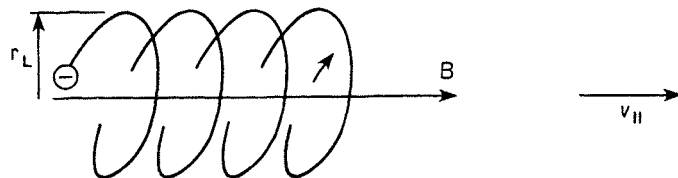


FIGURE 7. Trajectory of a (negatively) charged particle in a constant magnetic field.

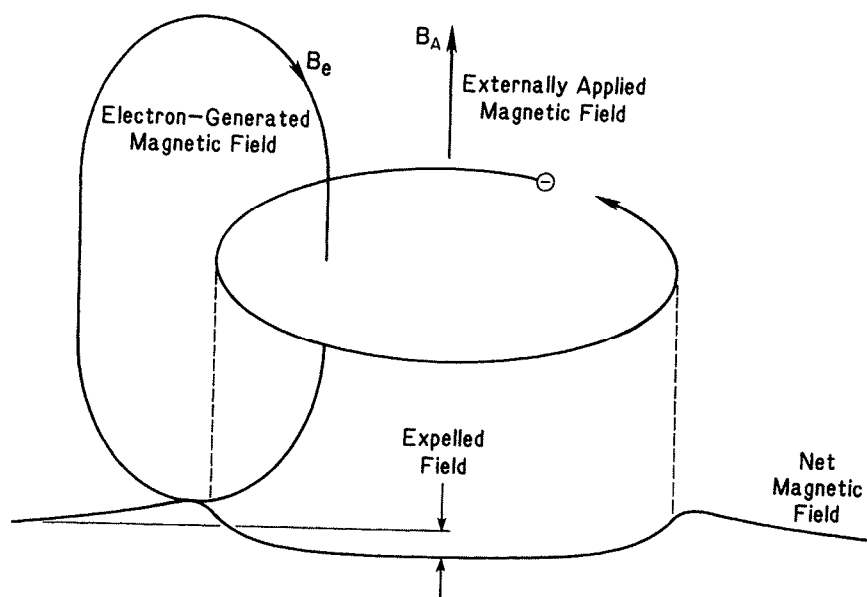


FIGURE 8. The magnetic field generated by the circling electron is oppositely directed to the applied  $B$  inside the orbit and in the same direction outside. The net field is thus reduced inside the orbit.

the *Larmor-*, *cyclotron-*, or *gyro-frequency*, which are related by

$$r_L = \frac{v_{\perp}}{\omega_c}. \quad (5)$$

The circular motion of the charged particle produces a dipole magnetic field in such a way as to reduce the strength of the field inside the circular orbit and to increase it outside (Fig. 8). Then one can view the circular motion as being caused by a higher magnetic pressure on the outside of the orbit. This property of a charged particle or a plasma to partially expel magnetic fields from their vicinity (interior) is called *diamagnetism*. The dipole field has a strength called the *magnetic moment* equal to

$$\mu = \frac{qv_{\perp}r_L}{2c} = \frac{mv_{\perp}^2}{2B}. \quad (6)$$

Another convenient picture of the motion is to separately consider the circular (cyclotron) and linear motions. By ignoring the cyclotron motion one has the *guiding center motion* remaining. This nearly linear motion is a worthwhile concept if the cyclotron radius is small compared to the other

characteristic dimensions. And so it is of most use for electrons whose Larmor radii are small because of their small mass.

C. E-PERPENDICULAR TO B

If **E** and **B** are parallel to each other, there is little change in a particle's motion from the above description. That is, a particle will accelerate along **E** and **B** and have an unchanging circular motion around them.

If **E** and **B** are perpendicular, however, a new effect takes place that is contrary to most everyday experiences, except that of the common toy top. What happens is that the charged particle starts to accelerate parallel to **E** until its velocity is large enough for the magnetic force to bend it. The bend becomes so large that the particle ends up moving in a direction that is perpendicular to both **E** and **B** (Fig. 9). Similarly, a spinning toy top, if pushed by a finger or by gravity, responds by precessing perpendicular to both the applied force and its axis of rotation, and not by falling over.

So the motion of the charged particle is the sum of three distinct motions: cyclotron motion around **B**; linear motion along **B**; and a drift

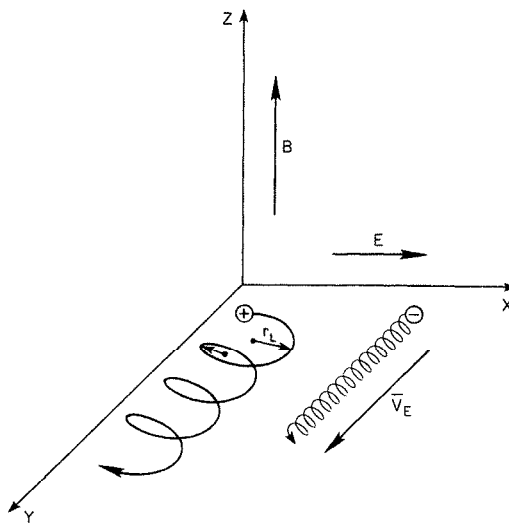


FIGURE 9. Drift of a charged particle in the presence of crossed **E** and **B** fields. Both electrons and ions drift in the same direction and at the same speed. Note that the Larmor radius changes as the particle gains and loses energy from the electric field. It is this difference in Larmor radius that causes the drift.

I A. Cohen

Net  
Magnetic  
Field

Directed to  
is reduced

(5)

magnetic  
circular  
circular  
e of the  
y expel  
m. The

(6)

der the  
motion  
ion is a  
e other

perpendicular to both  $\mathbf{B}$  and  $\mathbf{E}$ . The  $\mathbf{B}$ -parallel and  $\mathbf{B}$ -perpendicular (drift) motions now comprise the guiding-center motion.

Integrating the equation of motion for this case is more complicated than in the previous paragraphs. Instead, one can take the vector cross-product of  $\mathbf{B}$  with the Lorentz law, Eqn. (1), ignoring the  $d\mathbf{v}/dt$  term, which describes the cyclotron motion. Then one obtains for the transverse component of the velocity (the drift velocity)

$$v_E = c \left( \frac{\mathbf{E} \times \mathbf{B}}{B^2} \right). \quad (7)$$

This drift velocity is independent of the particle's energy, charge, and mass because the electric and magnetic forces are both proportional to a particle's charge and independent of a particle's mass. Though a heavy particle has a larger gyroradius, its cyclotron frequency is slower by the same amount so the gain and loss of energy from the electric field during each cycle are balanced.

#### D. NON-UNIFORM FIELDS AND OTHER FORCES

The same derivation could have been carried out for a different force  $\mathbf{F}$  acting on a charged particle in a  $\mathbf{B}$  field. The result can simply be obtained by replacing  $\mathbf{E}$  by  $\mathbf{F}/q$ , the equivalent electric field. The classic example most quoted is that of a charged particle in crossed magnetic and gravitational fields (Fig. 10a). The result is a drift velocity of magnitude  $cmg/qB$ , where  $g$  is the gravitational acceleration. This drift does depend on charge and mass because the gravitational force does not depend on charge but does depend on mass. Charges separate and the heavier particles drift faster. Hence, a net current flows, in contrast to the  $\mathbf{E} \times \mathbf{B}$  case.

Another drift would occur if the particle experiences a force due to a pressure gradient,  $\nabla p$ . This would arise in a plasma with temperature or density gradients. The resulting drift is called the diamagnetic drift and has a velocity equal to

$$v_D = \frac{c \nabla p \times \mathbf{B}}{qnB^2}. \quad (8)$$

Similarly, the drift resulting from gradients or curvature in the  $\mathbf{B}$  field itself can be written down immediately after identifying the forces they cause. A charged particle moving along a curved field line (Fig. 10b) feels a centrifugal force of magnitude  $mv_{\parallel}^2/R_c$ , where  $R_c$  is the radius of curvature of the field. And magnetic field gradients (Fig. 10c) cause a force equal to



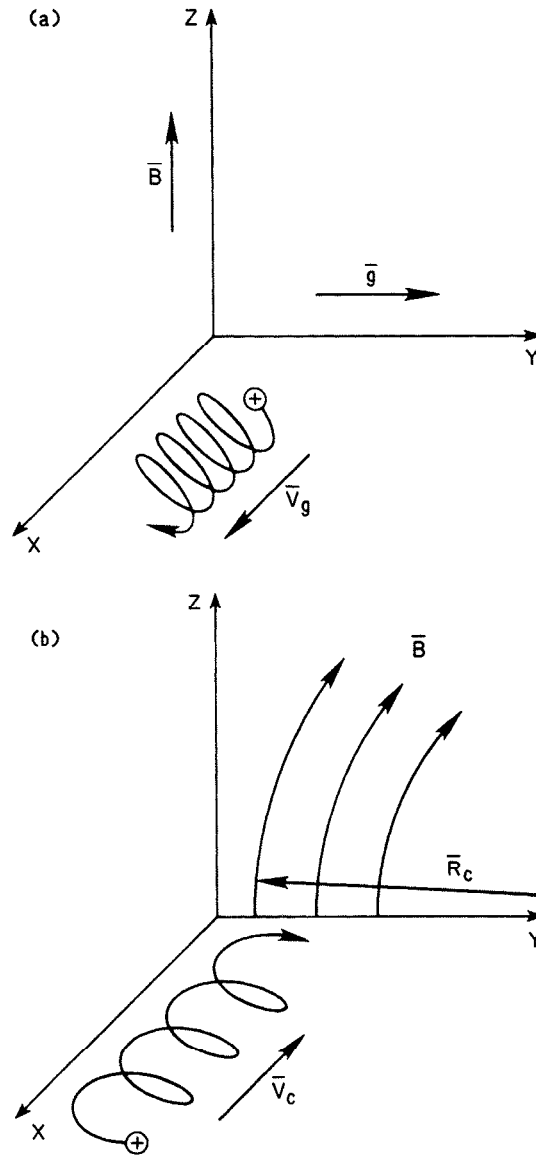


FIGURE 10. Drift motion of positively charged particles under the combined influences of a magnetic field and a) gravity, b) curved magnetic field, and c) magnetic field with a gradient (continued on next page).

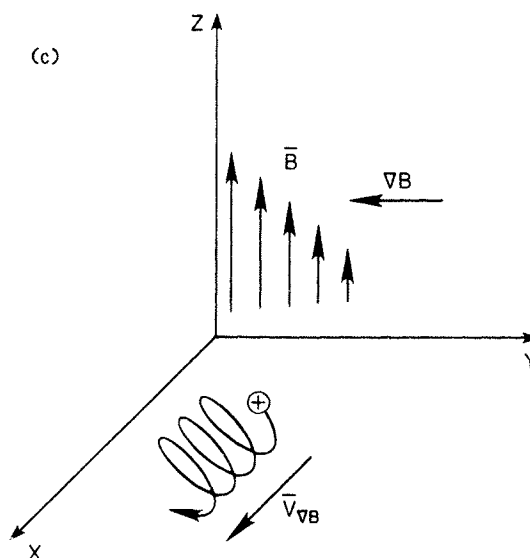


FIGURE 10c. Continued from previous page.

$\mu \nabla \mathbf{B}$ . Hence the drifts are:

$$v_G = \pm \frac{v_{\perp} r_L \mathbf{B} \times \nabla \mathbf{B}}{B^2} \quad (9)$$

and

$$v_c = \frac{mv_{\parallel}^2 \mathbf{R}_c \times \mathbf{B}}{qB^2 R_c^2}. \quad (10)$$

In contrast to the  $\mathbf{E} \times \mathbf{B}$  drift, these depend on a particle's mass, charge, and energy. The more massive a particle, the faster it drifts. This is another counter-intuitive property of plasmas. Generally one expects the electrons, the lighter particle, to carry all the electrical currents. Not so. The ions can play a dominant role in current flows.

A non-uniform electric field will alter the drift velocity by giving weight to the time the particle spends in the regions of different field strength and direction. The result for a sinusoidally varying electric field with a periodicity distance  $d$  is that the drift is proportional to the usual  $\mathbf{E} \times \mathbf{B}$  drift times  $(1 - r_L^2/4d^2)$ . This is called a finite Larmor radius correction because of the presence of  $r_L$  in the equation. This is different for each species and may cause charge separation and thus plasma waves.

E. TIME-VARYING FIELDS

When the electric field varies in time the drift is modified. One can again understand the motion from a microscopic picture. Each time the field "turns-on" the particle slowly accelerates parallel to  $\mathbf{E}$  and then the  $\mathbf{E} \times \mathbf{B}$  drift develops. When the electric field reverses the processes again occur, but with the drifts in the opposite directions. This can be seen quantitatively from the following derivation (Fig. 11a and b). The magnetic field is along the z-axis; the electric field is along the y-axis. The equations of motion for the x and y directions are:

$$\ddot{x} = \omega_c \dot{y} \tag{11a}$$

and

$$\ddot{y} = \frac{qE}{m} - \omega_c \dot{x}. \tag{11b}$$

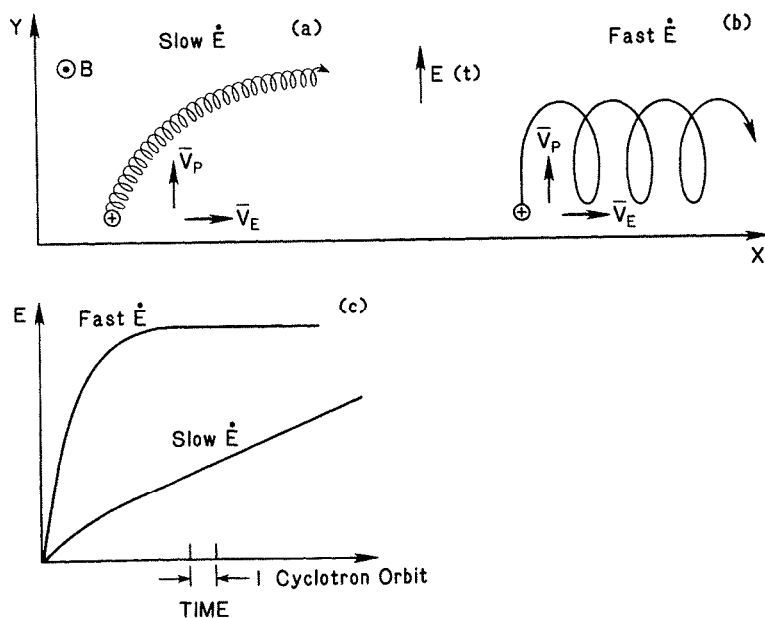


FIGURE 11. Polarization drifts for positively charged particles when  $\mathbf{E}$  increases monotonically with time. If  $\mathbf{E}$  increases slowly, the Larmor radius is unchanged. Two drifts develop: the  $\mathbf{E} \times \mathbf{B}$  drift and the polarization drift (parallel to  $\mathbf{E}$ ). When  $\mathbf{E}$  increases at a fast rate, relative to the period of the cyclotron motion, the Larmor radius grows as the particle gains energy from the field. Again two drifts develop. Note that when  $d\mathbf{E}/dt = 0$  the polarization drift also is 0.

By differentiating (11a) and substituting in (11b) and vice-versa, the equations can be made separable yielding,

$$\ddot{x} + \omega_c^2 x = \frac{q\dot{E}\omega_c}{m} \quad (12a)$$

and

$$\ddot{y} + \omega_c^2 y = \frac{q\dot{E}}{m}, \quad (12b)$$

which have solutions

$$\dot{y} = -v_{\perp} \sin(\omega_c t) + \frac{mc^2\dot{E}}{qB^2} \quad (13a)$$

and

$$\dot{x} = +v_{\perp} \cos(\omega_c t) + \frac{cE}{B}. \quad (13b)$$

It is now easy to identify the  $\mathbf{E} \times \mathbf{B}$  drift motion in the x-direction and the polarization drift in the y-direction,  $mc^2\dot{E}/qB^2$ . The orbit shapes will vary depending on the rate of change of the electric field. Figure 11 shows two cases, both for monotonically increasing fields, not oscillating ones. In Fig. 11b the rapidly changing intense field increases the Larmor radius because it adds an appreciable amount of energy to the particle in a time faster than the cyclotron period.

The polarization drift is in opposite directions for oppositely charged particles. Hence charge separation occurs. Again the more massive particle carries the current.

## F. ADIABATIC INVARIANTS

A similar derivation carried out for slowly varying magnetic fields shows that no additional drift arises. Instead the Larmor radius grows or shrinks, depending on whether  $B$  decreases or increases. This is associated with a decrease or increase of the particle's transverse energy (see Eqn. (4)). The change is such that the magnetic moment is unchanged. So  $v_{\perp}^2$  increases proportional to  $B$ .

The magnetic moment is called the *first adiabatic invariant*. It is constant as long as changes in  $\mathbf{E}$  or  $\mathbf{B}$  occur slowly compared to a cyclotron orbit. Its constancy reflects the symmetry and periodicity of the cyclotron orbit.

Sitting in the particle's frame-of-reference, a change of  $\mathbf{B}$  can come from a change in its position as well as a change in the local field strength. Recall that static magnetic fields add no energy to a particle. It is then clear that the change in perpendicular energy must be accompanied by an equal but opposite change in parallel energy. So if a particle moves into a region of

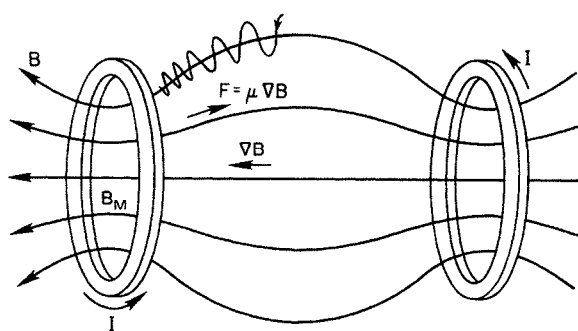


FIGURE 12. Magnetic mirror formed by two coaxial coils with co-directed currents,  $I$ . As a charged particle approaches a region of higher  $B$ , its perpendicular energy grows at the expense of its parallel energy. Reflection will occur if  $B$  reaches a high enough value. Note that the Larmor radius shrinks as the particle moves into a region of higher  $B$ .

increasing  $B$ , it will continue to gain perpendicular energy at the expense of its parallel energy. At some point it may have lost all its parallel energy. With  $\nabla B$  still causing a force on the particle it is reflected. This property of spatially varying magnetic fields is called the *mirror effect* and forms the basis for many plasma confinement configurations (Fig. 12). For the mirror to “work,” the particle must start with sufficient perpendicular energy because the mirror force only acts on the magnetic moment ( $F = \mu \nabla B$ ). From conservation of energy and  $\mu$  we can show that a particle starting from a region of magnetic field strength  $B_0$ , will only be reflected in the region of higher field if its pitch angle,  $\theta = v_{\parallel}/v_{\perp}$ , is less than

$$\frac{B_0}{B_M} = \sin^2 \theta = (R_M)^{-1} \quad (14)$$

where

$R_M$  = the mirror ratio, and  
 $B_M$  = the maximum field strength.

The underlying principles for these statements are the laws of conservation of energy and angular momentum. These are very powerful tools when a physical situation has symmetry. For example, calculations of cosmic ray trajectories in the earth’s vicinity are easy because of the size of the earth coupled with the symmetry of its magnetic field. The symmetry is such that other invariants of the motion, the so-called second and third adiabatic invariants, help to solve the problem. They are based on the symmetry and periodicity of the large-scale motion around the earth (bouncing back and forth between the magnetic mirrors at the poles and circulating around the equator), not just of the cyclotron orbit. In plasma processing equipment,

however, collisions are too frequent and the size of the apparatus too small to allow undisturbed orbits around the material structures. Thus, the only useful invariant is the first.

### G. SUMMARY OF PARTICLE DRIFTS

It is easiest to use the information just presented on the drift motions by rewriting their equations expressed in practical units. The parameters, symbols and practical units for this are listed next.

These drift velocities should be compared with the thermal velocities of the ions and electrons, which are

$$v_t = (2W/m)^{1/2} = 5.9 \times 10^7 (W)^{1/2} \text{ cm/s} \quad \text{for electrons} \quad (16a)$$

$$= 1.4 \times 10^6 (W/M)^{1/2} \text{ cm/s} \quad \text{for ions.} \quad (16b)$$

| Parameter              | Symbol          | Practical Units       |
|------------------------|-----------------|-----------------------|
| magnetic field         | $B$             | gauss                 |
| electric field         | $E$             | volts/cm              |
| gravitational constant | $g$             | $\text{cm/s}^2$       |
| ion mass               | $M$             | amu (proton mass = 1) |
| charge                 | $q$             | -1 for an electron    |
| radius of curvature    | $R_c$           | cm                    |
| gradient scale length  | $R_G$           | cm                    |
| temperature            | $T$             | electron volts        |
| parallel energy        | $W_{\parallel}$ | electron volts        |
| perpendicular energy   | $W_{\perp}$     | electron volts        |
| total kinetic energy   | $W$             | electron volts        |
| cyclotron frequency    | $\omega_c$      | /sec                  |

| Drift         | Symbol                  | Value (cm/s)                                   |
|---------------|-------------------------|--|
| $E \times B$  | $v_E$                   | $10^8 E/B$                                     |
| diamagnetic   | $v_D$                   | $10^8 T/R_G B$                                 |
| gravitational | $v_g$                   | $10^{-4} gM/B$                                 |
| curved B      | $v_c$                   | $2 \times 10^8 W_{\parallel}/R_c B \quad (15)$ |
| grad B        | $v_G$ or $v_{\nabla B}$ | $10^8 W_{\perp}/R_G B$                         |
| polarization  | $v_p$                   | $v (\omega/\omega_c)$                          |

for  $E = E \cos(\omega t)$

#### IV. Plasma Parameters

The preceding section described the motions of individual particles under the joint influences of electric and magnetic fields. Nowhere was there a need to consider the presence of a group of particles. In this section we describe the salient properties of a group of charged particles. Some of these properties are so general, e.g., temperature and pressure, that they apply to all states of matter; others concern the plasma state only, e.g., plasma oscillations.

##### A. TEMPERATURE, DENSITY, AND PRESSURE

The concept of temperature is a very precise one. Only if a collection of particles exists *and* only if that collection has a certain distribution of particle energies, may a temperature be defined. That distribution is called a Maxwellian and its shape is shown in Fig. 13. It is not necessary—in fact it is a rarity—for plasmas to be exactly Maxwellian. Even the average energy of particles may dramatically vary between different locations in the containment vessel. In spite of all this, the concept of temperature, or at least of an average energy, is useful in a local description of plasmas.

Note in Fig. 13 that there are no particles with zero energy. There is also a clear maximum in the distribution. Most particles have energies within a few times the most probable energy. It is usually the particles in the tail, however, with about four times the most probable energy, that dominate the physical processes. There are two reasons for this. First, these particles are twice as fast-moving as the others, hence they interact more frequently; and more importantly, most physical processes, ionization for example, are near threshold at the low energies (5 to 10 eV) characteristic of plasma processing discharges. Hence small changes in energy make exponential changes in reaction rates. This is one reason why great efforts are made to increase the temperature of plasmas. A two-fold increase in the electron temperature can increase the reactivity ten-fold. In Section IV.D, we evaluate this quantitatively to see if there is an upper limit to the desired temperature.

A second important parameter describing a plasma is its density. This too is of critical importance in determining reaction rates. As stated earlier, the densities of positive and negative charges are locally balanced, usually to better than 1%. Across a plasma device, though, the densities can vary a hundred-fold or more. One usually aims at keeping the density high near the work surface if it is desired to have plasma bombardment of that surface. But there are applications where plasma bombardment is undesirable, such as when lattice damage or arcing might occur. Figure 14 shows

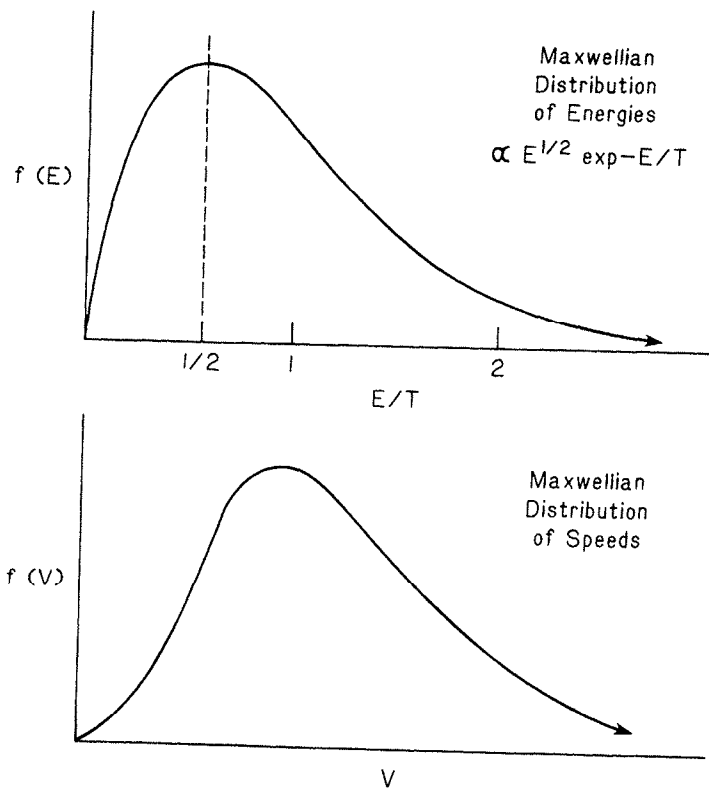


FIGURE 13. Maxwellian distributions of energy and speed.

typical ranges for the temperatures and densities of the various species in processing plasmas. Note that the ion energies in the sheath may be very high.

The product of plasma density times temperature gives the plasma pressure. This quantity is a measure of how well used is the energy provided to form the plasma. The *energy confinement time* is the ratio of the stored energy (plasma pressure times the plasma volume) to the input power. As will be seen later by an application of this concept, different methods of plasma formation and confinement place quite different requirements on the power supplies used to generate and to maintain the plasmas and also affect where the input power is ultimately deposited.

In the ensuing sections the reader should carefully note the use of  $k_B$  denoting Boltzmann's constant and  $k$  denoting the wavenumber of a periodic disturbance in the plasma.



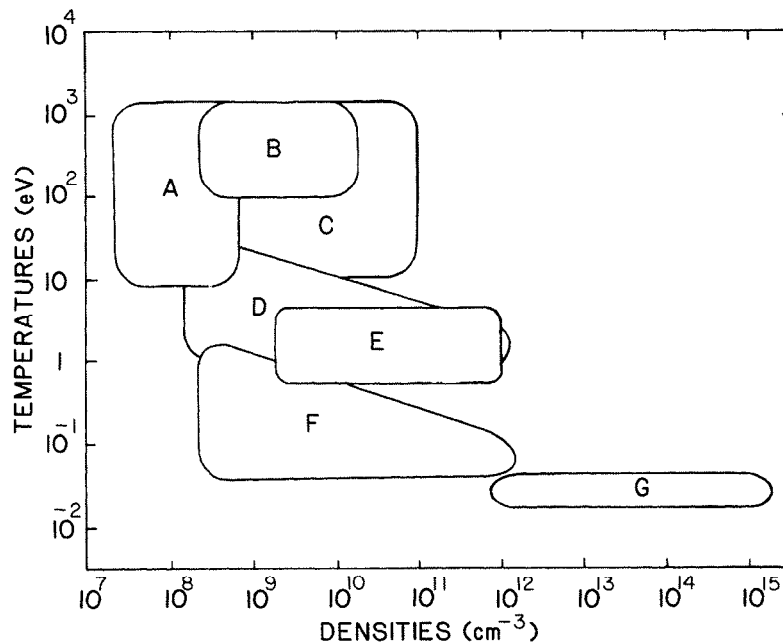


FIGURE 14. Ranges of temperatures and densities of particles typically present in process plasmas: A = secondary electrons accelerated through sheath (cathode), B = ions backscattered from cathode (possibly neutralized), C = ions accelerated towards cathode, D = electrons in main plasma, E = Franck-Condon ions and neutrals, F = ions in main plasma, G = neutral atoms and molecules.

### B. DEBYE LENGTH AND PLASMA FREQUENCY

Consider a collection of charged particles arranged in a slab, with equal numbers of each charge. Try to displace the positive charges to the right and the negative ones to the left (Fig. 15). Energy is required to effect the separation. An electric field develops, which makes the separation of charges progressively more difficult. Now consider the particles as they try to separate by simply using their own thermal energy, not some externally supplied source. The distance they can separate depends on their thermal energy. When their thermal energy is all converted into potential energy they can separate no further. The potential energy,  $U = q\Delta\phi$ , may be derived from Poisson's equation for the potential

$$\nabla^2\phi = 4\pi(n_i - n_e)q, \tag{17a}$$

cies in  
e very

lasma  
vided  
stored  
er. As  
ods of  
its on  
d also

of  $k_B$   
of a

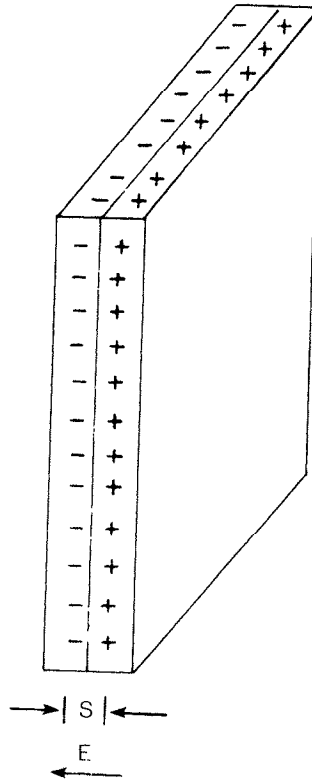


FIGURE 15. Collection of charged particles in a slab. The positive particles were displaced from the negative. A strong electric field results, which will force the two sets of particles back toward each other.

which, for a separation  $s$ , gives

$$\Delta\phi = -2\pi nqs^2. \quad (17b)$$

This is the potential energy change,  $q\Delta\phi$ , as a function of the separation of the charges. By equating the available thermal energy ( $k_B T_e/2$  because of the 1-dimensional motion) with the potential energy, we can solve for the maximum distance,  $\lambda_D$ , by which the charges may separate from each other before the restoring force of the electrostatic field pulls them back together again. This distance is the Debye length,  $\lambda_D$ .

$$\lambda_D = \left( \frac{k_B T_e}{4\pi n_e q^2} \right)^{1/2}. \quad (18)$$

Another way to calculate the Debye length is by asking how charges rearrange themselves around a test particle in response to its electric field. After finding the distribution of charges, we again would use Poisson's equation to see how much the Coulomb field is reduced. The answer we would obtain is that the electric field is reduced to  $1/e$  of its Coulomb value in a distance equal to the Debye length. Thus, the electric field does not penetrate into a plasma further than one Debye length. We shall discuss this more in regards to the presheath and to magnetized plasmas.

We are now able to find out how many particles are still affected by the shielded field of the test particle. This can be estimated by calculating the number of particles within a sphere of radius  $\lambda_D$ .

$$N_D = \frac{n_e 4\pi \lambda_D^3}{3} = \frac{(k_B T_e / q^2)^{3/2}}{3(4\pi n_e)^{1/2}} \quad (19)$$

This number, commonly called the *plasma parameter*, must be large (more than 100) for collective effects to be important.

There are two reasons for showing the first derivation. First, the mathematics is simpler. And second, it naturally leads into the next topic, the plasma frequency,  $\omega_{pe}$ . As just stated, when the two slabs of charge are separated (Fig. 15), a restoring force is developed. This pulls the charges back toward each other. They accelerate and then pass through their equilibrium positions and separate in the opposite sense. Now the positive charges are to the left and the negative to the right. It is easy to estimate the frequency of this motion. It is simply the inverse of the time it takes particles to move the Debye length at their thermal velocity.

$$\omega_{pe} = \frac{v_{e\perp}}{\lambda_D} \quad (20)$$

Consider the influence of a material object on the plasma with a sheath developed at the interface. For convenience, choose a metal sphere floating freely in the plasma. At the instant of its introduction it has no net charge. But the electrons flow rapidly into it because they are much faster than the more massive ions. The electron flow progressively charges the sphere to a negative potential. When the value of this potential exceeds a few times the electron temperature, most electrons are repelled by the field. Soon a steady state is reached where the greatly reduced flow of electrons is balanced by the flow of ions. This is called the *floating potential*,

$$\phi_f = 0.5(k_B T_e / q) \ln \left[ \left( 2\pi \frac{m_e}{m_i} \right) \left( 1 + \frac{T_i}{T_e} \right) \right]. \quad (21)$$

The ions that provide the charge to balance the electron flow originate deep in the plasma from a region called the *presheath*. Its length may be 100s of Debye lengths. The condition of charge neutrality in the plasma requires that the ions are accelerated from the presheath into the sheath up to a velocity,  $c_s$ , called the *sound speed*,

$$c_s = \left( \frac{k_B T_e + k_B T_i}{m_i} \right)^{1/2}. \quad (22)$$

To arrive at the sheath with this velocity, the potential drop,  $\Delta\phi_{ps}$ , integrated along the entire presheath, must be  $\sim 0.5 T_e$ . (More detailed theories of  $c_s$  and  $\phi_f$  change the coefficients of Eqns. (21) and (22) by up to 40%, depending on geometry, the plasma equation-of-state, and other factors.)

It is clear from this discussion that the plasma is severely perturbed in the immediate vicinity of the object. For example, there is no return flow of electrons and ions from the sphere. The electron and ion densities in the sheath do not balance because of the electric field that has developed (Fig. 16). The distance of the perturbation is approximately five times the Debye length. And the size of the potential drop is 4.7 times the electron temperature for an argon plasma (Eqn. (21)). Thus, the ions that reach the surface will have an energy equal to what they have in the plasma plus what they have gained in passing through the presheath and sheath,  $(4.7 + 0.5)k_B T_e$ .

With these three concepts now in hand, it is instructive to review the single-particle approach to see what other effects (beyond increasing the ion energy) the plasma presheath and sheath may have on ions hitting surfaces. For example, consider a magnetized isothermal plasma with  $\mathbf{B}$  parallel to a metal surface. Ions that enter the sheath—later we will describe how they might be transported across the magnetic field—will find themselves in a region of crossed electric and magnetic fields. Will they be rapidly accelerated and hit the surface at normal incidence before the  $\mathbf{E} \times \mathbf{B}$  drift develops, or will they be so deflected by the drift that they skim along the surface only to hit it at a grazing angle? This has consequences to both the sputtering rate and erosion profile. Though a detailed calculation of particle trajectories through the sheath is necessary to answer these questions accurately, we can get an approximate answer by simply comparing the  $\mathbf{E} \times \mathbf{B}$  drift velocity and the thermal velocity. Setting Eqns. (7) and (16) equal gives

$$v = \left( \frac{k_B T}{2m} \right)^{1/2} = v_E = \frac{cE}{B}.$$

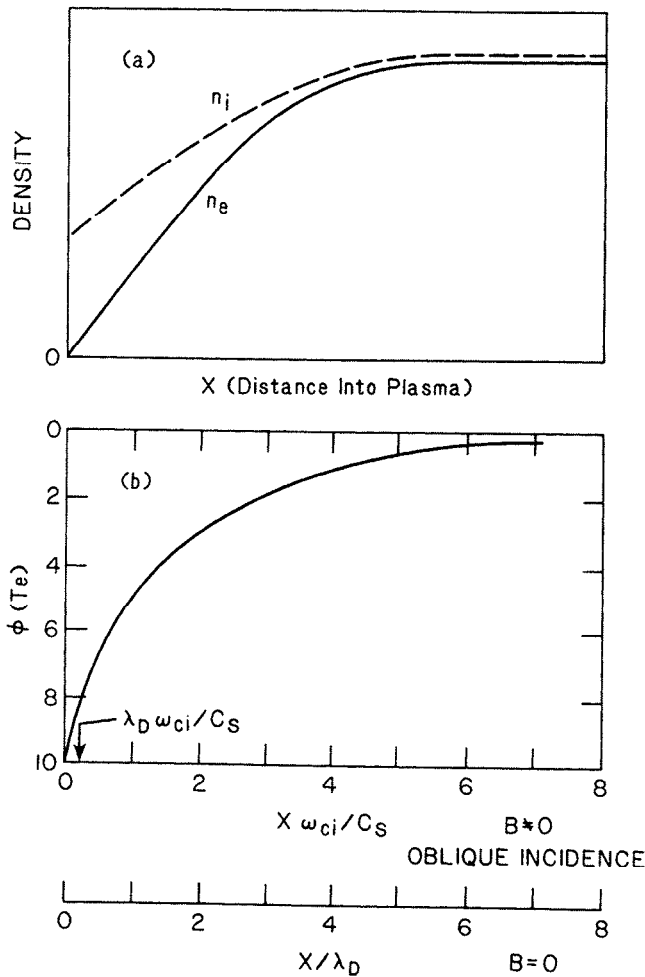


FIGURE 16. a) The electron and ion densities in the sheath region of plasma. b) The potential distribution is shown with two different distance scales: one is to be used for unmagnetized plasmas (or when  $B$  is normal to the surface); the other is for when  $B$  intersects the surface at an oblique angle. The value of the potential at the surface depends on the ion mass and temperature (see Eqn. 21).

In the sheath the electric field is approximately the potential energy change,  $U \cong 5kT_e$ , divided by the sheath thickness,  $\sim 5\lambda_D$ . So using Eqn. (19) for  $\lambda_D$ , this can be rearranged to yield

$$\frac{B^2}{8\pi} = nm_i c^2. \quad (23)$$

From Eqn. (23), we can determine the conditions for which the  $E \times B$  drift velocity will be more important than the thermal motion or the sheath-induced velocity (since both have the same dependence on  $T$ ). This occurs when the magnetic energy,  $B^2/8\pi$ , is less than the Einstein self-energy,  $nm_i c^2$ . Using standard parameters for a magnetron discharge, i.e.,  $B = 1000$  g and argon ions, we find that the critical density above which  $v_E$  may cause glancing ion impacts is about  $10^6 \text{ cm}^{-3}$ . The single-particle picture is open to question if the orbit size,  $r_L$ , exceeds the sheath size. The comparison is made using Eqns. (4) and (19),

$$\lambda_D = r_L,$$

which upon substitution and rearrangement gives:

$$\frac{B^2}{8\pi} = nm_i c^2.$$

That is, the same conditions satisfy both requirements. If the density is below the critical value, then the ion cyclotron radius is smaller than the sheath thickness and the single particle picture is correct. Then the  $\mathbf{E} \times \mathbf{B}$  drift is less important than the thermal motion. But magnetrons operate at densities of about  $10^{11} \text{ cm}^{-3}$ , well above the critical value. So the application of the drift equations is not as simple. The ions do not stay in the sheath long enough for the  $\mathbf{E} \times \mathbf{B}$  drift to fully develop. All this was based on the assumption of an isothermal plasma. Usually the ions are colder than electrons in these devices. Hence their gyroradii may be smaller. Again, to answer these questions accurately, one should calculate the forces on an individual ion as it enters and moves through the sheath. This could be done with the Lorentz force law, Eqn. (1). One calculation, see Chodura in Ref. 10, shows the angle of incidence (with respect to the surface-normal) of ions is about 1/2 the angle of incidence of the magnetic field. (The presheath has much larger dimensions; hence, the  $\mathbf{E} \times \mathbf{B}$  drift does develop and ions are accelerated parallel to the surface.)

In summary, evaluation of ion trajectories based on the single particle equations of motion in a magnetized plasma shows that ions are accelerated in both the sheath and presheath to a net velocity, which is oblique to metal surfaces when the plasma density exceeds about  $10^6 \text{ cm}^{-3}$ . Detailed calcula-

tions are required for a particular geometry and set of plasma parameters to quantify the distribution of angles of impact.

Before leaving the subject of magnetized plasmas, it is important to note the effects of the magnetic field on the sheath. If the magnetic field is normal to the surface there is no change in the sheath. But an obliquely incident magnetic field does change things considerably. Mainly, this is due to the fact that the electric field, set up by the initial electron flow to the object, now has to overcome the Lorentz force on the ions in addition to the ion inertia. The net result is that the floating potential changes little, but the sheath extends further into the plasma by a distance equal to several ion gyroradii. However, the appropriate ion gyroradius to use is that of the ion with an energy obtained from the  $\mathbf{E} \times \mathbf{B}$  drift motion. This second part of the sheath is termed the magnetic part; the first is the electrostatic (see Fig. 16b). This reduces the rigidity of the requirement we arrived at in Eqn. (23).

### C. SKIN DEPTH AND DIELECTRIC CONSTANT

We have just seen that a plasma will shield its interior from an externally applied static electric field. It also reduces the distance over which the electric field from individual charges in the plasma has an effect. But what about the penetration of time-varying fields, i.e., waves? There are two general classes of waves: electrostatic (also called longitudinal) and electromagnetic (also called transverse). The first have their electric field parallel to their direction of propagation. These types of waves cannot propagate in empty space. They need a medium, like a plasma, to support their motion. The second have their electric field perpendicular to their direction of propagation. Light waves are a member of this class, and they can obviously propagate through vacuum.

It is instructive to compare the derivations of the penetration depth, the *skin depth*, for these two different types of waves. For the longitudinal waves, we will start with the force law. To Eqn. (1) we must add a term that denotes the pressure caused by the bunching of charges. After all, the longitudinal wave is a pressure wave generated when the applied electric field causes electrons to bunch. Magnetic forces are unimportant. For simplicity we will consider only motion in one direction, the x-direction. Then the force equation is

$$\frac{mn \partial v_1}{\partial t} = -qn_0 E - 3T \frac{\partial n}{\partial x}. \quad (24)$$

We now look for wave solutions with the standard form,  $\exp(i(kx - \omega t))$ .

(Perturbed quantities have subscript 1). Poisson's equation gives

$$\nabla^2 \phi = 4\pi(n_i - n_e)q$$

or

$$-\nabla E = ikE = 4\pi qn_1 \quad (25)$$

and the equation of continuity gives

$$\frac{\partial n}{\partial t} = -n_0 \nabla v_1 \quad (26a)$$

or

$$i\omega n = n_0 ikv. \quad (26b)$$

Substituting (25) and (26) into (23) gives

$$\omega^2 = \omega_{pe}^2 + \frac{3}{2}k^2 v_i^2 \quad (27)$$

or

$$k = 2\omega_{pe} \frac{\left(\frac{\omega^2}{\omega_{pe}^2} - 1\right)}{3v_i}. \quad (28)$$

For  $\omega \ll \omega_{pe}$ ,

$$k \approx \frac{2i}{3\lambda_D} \quad (29)$$

or  $\delta_{||}$ , the skin depth for low frequency longitudinal waves, is

$$\delta_{||} = \frac{3\lambda_D}{2}. \quad (30)$$

So longitudinal waves with frequencies less than the electron plasma frequency only penetrate about a Debye length into a plasma. This is because the electrons in the plasma are able to move fast enough to shield out the relatively slowly varying longitudinal electric field.

We now consider transverse waves, again with frequencies less than the plasma frequency. The difference between this case and the previous can be seen in Fig. 17. The electrons are pushed up and down in sheets in the plasma. No bunching develops to shield the electric field. Instead the flowing electrons generate a magnetic field to counter that of the electromagnetic wave. To analyze this situation, start with Maxwell's equations in a dielectric medium,

$$\nabla \times D = -\frac{1}{c} \frac{\partial H}{\partial t} \quad (31)$$



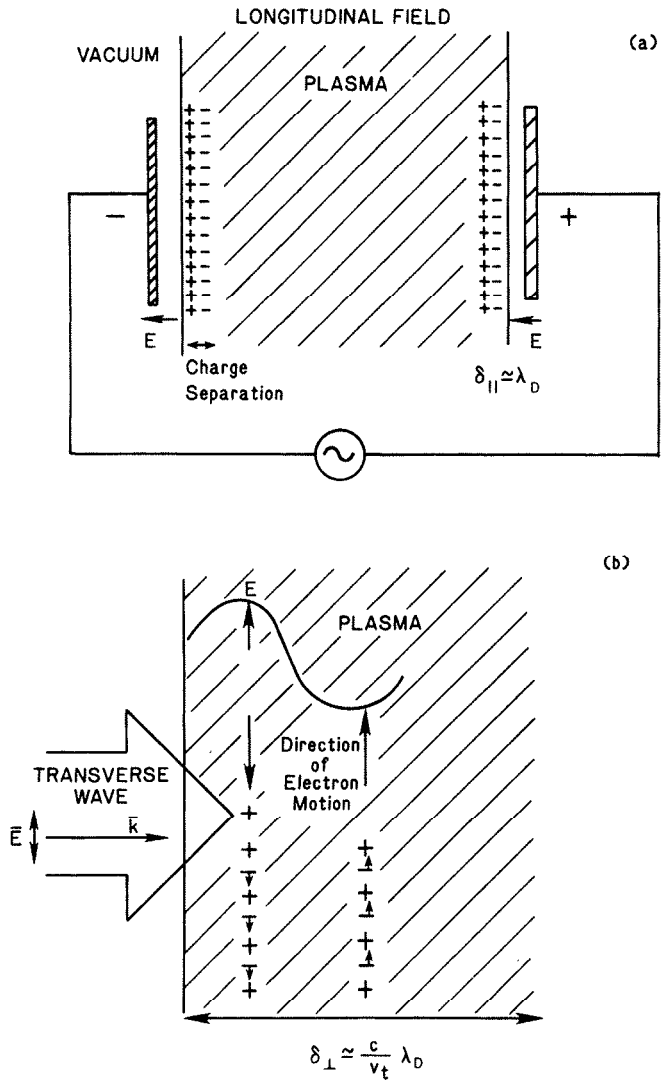


FIGURE 17. Penetration of low frequency longitudinal a) and transverse b) waves into plasmas. A longitudinal field causes charge separation at the plasma surface. The transverse wave does not and hence may penetrate further.

and

$$\nabla \times H = -\frac{1}{c} \frac{\partial D}{\partial t} + \frac{4\pi J}{c}, \quad (32)$$

where  $D = \epsilon E$  and  $B = \mu_D H$ .  $\epsilon$  is the dielectric constant and  $\mu_D$  is the magnetic permeability  $\approx 1$ . Take the curl of both sides of Eqn. (31). Use the facts that

$$J = -n_0 e v_1 \quad (33)$$

and

$$\frac{m \partial v_1}{\partial t} = \frac{q E_1}{i m \omega}. \quad (34)$$

This gives

$$k = \omega_{pe} \frac{\left( \frac{\omega^2}{\omega_{pe}^2} - 1 \right)^{1/2}}{c}, \quad (35)$$

which for  $\omega \ll \omega_{pe}$  yields

$$k \approx \frac{i \omega_{pe}}{c} \quad (36)$$

or

$$\delta_{\perp} = \frac{c}{\omega_{pe}} = \frac{c \lambda_D}{v_t}. \quad (37)$$

So the penetration of transverse waves into plasmas is much further than longitudinal waves. Typically the ratio  $c/v_t$  is 1000, so transverse waves may penetrate tens of centimeters into the plasma before they are absorbed (or reflected). This offers an important choice when waves are being considered for heating or sustaining plasmas. For example, does the process require a high energy content in the edge (plasma sheath) for sputtering, or is it better to deposit the energy further in the plasma where it may preferentially be used for ionization and molecule fragmentation?

The inclusion of a magnetic field into the preceding calculations increases the complexity of the analysis. Some results will be presented in a later section on waves. Here, however, a more basic concept is presented, the dielectric constant. This has close ties to the results just obtained on the strength of the electric field inside plasmas and on the drift motions described in the previous section.

Let us guess at the result. Because a magnetic field hinders the movement of charged particles, we expect that for large  $B$  both the charge bunching and the sheets of current (formed in response to the longitudinal and transverse waves respectively) will be reduced; hence the shielding ability of

the plasma for both longitudinal and transverse waves will decrease. To see if this is true start again with Maxwell's equation,

$$\nabla \times B = \frac{4\pi J}{c} + \frac{\dot{E}}{c}. \quad (38)$$

The current can be divided into two terms: one that is the polarization current due to the changing  $E$  field,  $J_p$ ; the other containing all other currents,  $J_0$ . From Eqn. (14) one can write an expression for the polarization current (which is due mostly to ions)

$$J_p = n_0 q v_p = \frac{n_0 m_i c^2 E}{B}. \quad (39)$$

So Eqn. (38) becomes

$$\nabla \times B = \frac{4\pi J_0}{c} + \frac{\epsilon \dot{E}}{c} \quad (40)$$

where  $\epsilon$  is defined as

$$\epsilon = 1 + \frac{4\pi n m_i c^2}{B^2}. \quad (41)$$

This is nearly the same as Eqn. (23). Equation (41) was derived for low frequencies and  $E$  perpendicular to  $B$ . The point to be remembered is that  $\epsilon$  represents how much the strength of a time-varying transverse electric field of a wave is reduced inside the plasma.

#### D. COLLISIONS

Collisions take place when charged and/or neutral particles interact in the plasma and also when they impact the walls and structures of the containment vessel. Though most textbooks ignore the second type, these are so critical to plasma processing that a short review of the most important surface effects is included at the end of this section. This is a prerequisite for understanding the sustenance of plasma discharges presented in Section V.

In the following discussion we consider only positive ions. In many plasmas these overwhelmingly dominate. There are cases, however, particularly at high density or when electronegative atoms or molecules are present, that copious numbers of negative ions will exist. They modify the species that impact the anode and also substantially change plasma properties such as mobilities, diffusivities, sheaths, floating potentials, and so forth.

Collisions in the plasma have contrary roles. They can result in the birth or loss of ions, the transport or confinement of plasma, and the gain or loss of heat. In the next paragraphs qualitative arguments will be presented to support this statement followed by quantitative formulae.

The impact of an energetic electron on a neutral atom may result in the creation of an ion-electron pair. This process is energy dependent. As shown in Fig. 18, the ionization rate coefficient increases rapidly with electron energy to a maximum at about 100 eV and then falls slowly. Since most plasma processing devices have a low electron temperature, it is clear that a slight increase in  $T_e$  will result in a great increase in plasma production rate. The ionization rate coefficient,  $R_I$ , may be approximated by

$$R_I = \frac{2.5 \times 10^{-6} \eta_e (T_e/\chi) \exp(-\chi/T_e)}{(1 + T_e/\chi)} \text{ cm}^3/\text{s} \quad (42)$$

where

$T_e$  = electron temperature (eV)

$\eta_e$  = number of equivalent outer electrons (1 for H, 2 for H<sub>2</sub>)

$\chi$  = ionization potential (eV).

The exponential term in Eqn. (42) arises from the exponential in the Maxwellian velocity distribution function of the impacting electrons. This formula, a phenomenological fit, is only valid for  $\chi \geq T_e/30$ .

As hinted earlier, there may be unwanted effects if the plasma is too hot and too dense. Consider the case of Al sputtering by Ar. If the plasma density exceeds  $10^{13} \text{ cm}^{-3}$  and the temperature exceeds about 50 eV, the sputtered Al will be ionized close (within 1 cm) to where it has been sputtered away. Then, as positive ions, it would be attracted toward and redeposited on the negatively biased Al target plate, reversing the desired effect.

Electrons may reattach themselves to ions. The simple radiative recombination process is slow at plasma temperatures above 1 eV. Even at this low temperature, the recombination time for a plasma of density  $10^{11} \text{ cm}^{-3}$  is about 10 sec, which is much longer than the lifetime of particles in the plasma due to flow to the electrodes, for example. If the density is much higher or the temperature much lower, as might occur in high-pressure plasma processes, then recombination can be sped up to play an important role in plasma loss. An approximate formula to estimate the recombination rate coefficient,  $R_R$ , is

$$R_R = 1 \times 10^{-13} Z \frac{\chi}{T_e} \left( 0.4 + 0.5 \ln \frac{\chi}{T_e} + 0.4 \frac{\chi}{T_e} \right) \text{ cm}^3/\text{s}. \quad (43)$$

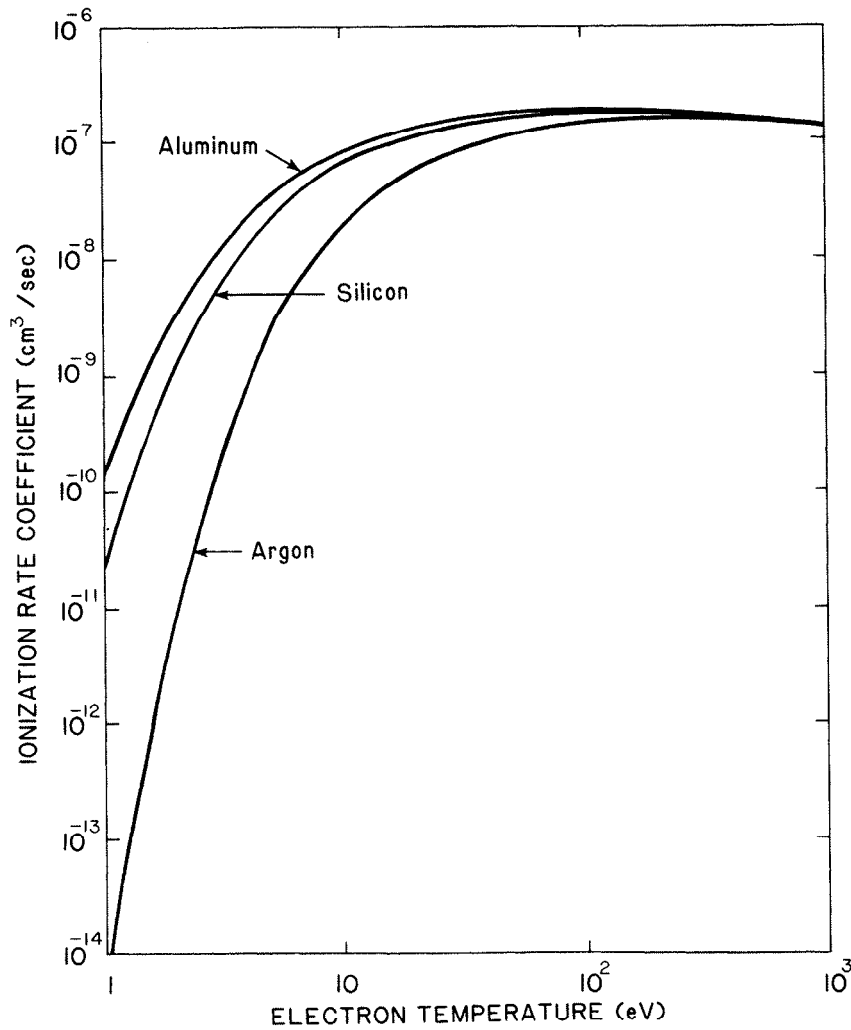


FIGURE 18. Ionization rate coefficient versus electron temperature for electron impact on Al, Ar, and Si.

The collision of an ion with a neutral will rarely result in the creation of a free electron. However, the exchange of an electron is highly probable. The rate coefficient of this process is nearly independent of energy and is about the same as for electron impact ionization,  $10^{-9}$  cm<sup>3</sup>/s. This phenomena can lead to the presence of energetic neutrals whose trajectories are unaffected by electric or magnetic fields. The importance of this to the etch profile is clear.

The second set of contrary effects deals with plasma confinement. For simplicity consider the case of an unmagnetized plasma (i.e., there is no external magnetic field applied) in a metal containment vessel. If the plasma density is low then the charged particles can freely stream to the walls where neutralization takes place (Fig. 19a). One way to reduce the rate of plasma loss is to increase the plasma density. Then collisions will convert the free-streaming situation into a diffusion-dominated one (Fig. 19b). One need not rely on charged-particle collisions to effect this improvement in confinement; neutral-charged particle collisions will do as well. The diffusion coefficient is approximately given by

$$D \cong \frac{\lambda_m^2}{\tau_m}, \quad (44)$$

where  $\lambda_m$  is the mean-free-path between collisions and  $\tau_m$  is the time between collisions. The mean-free-path will depend on whether it is charged-particle pair scattering or charged-neutral scattering that is more important.

The inclusion of a magnetic field into the problem completely alters the outcome. Consider an infinitely long cylinder with a uniform magnetic field parallel to its axis. The ions and electrons may flow freely along  $B$  but are constrained to remain within one Larmor radius of the field line on which they originate—unless, of course, they collide with other particles. Then they may jump one Larmor radius inward or outward (see Fig. 19c). So diffusive motion occurs again. But this time the “perfect” confinement of the magnetic field is degraded by collisions. If the collision is with a neutral, the neutral may move in an arbitrary direction relative to the field and the ion (or electron) then bounces in such a way to conserve total momentum. In short, the ion will probably bounce one Larmor radius and the ion density profile will expand diffusively. When two similar ions collide, the result may again be a single Larmor radius shift for each particle. But when one particle goes inward the other goes outward. There is a detailed balance and no net change in particle density. The classical collisions between charged particles of equal mass and charge do not contribute to particle diffusion. Ion-electron collisions do lead to diffusive transport, but at a slow

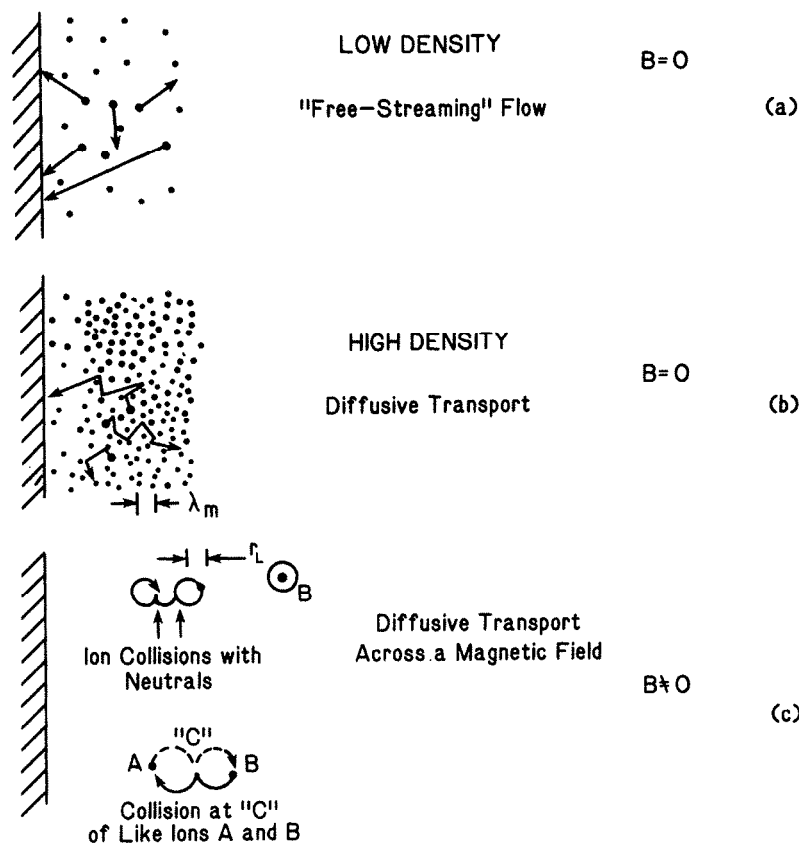


FIGURE 19. Plasma transport dominated by a) "free-streaming" flow, b) diffusive flow, and c) diffusion across  $B$  due to collisions. Note that in case c), collisions between like ions do not result in the net transport of particles. The inward displacement of one ion is exactly balanced by the outward displacement of the other.

rate because of the poor momentum transfer between particles of such disparate mass.

There is yet another type of "collision" that leads to transport. It is more accurately described by the term particle-wave interaction. Waves, or fluctuations in particle densities, result in fluctuations in electric field. The magnitude of the electric field is directly proportional to the electron energy, hence its temperature. This electric field may lead to an  $E \times B$  drift and particle loss. Surprisingly, a simple expression for the diffusion coeffi-

cient, derived by Bohm using very elementary arguments based on this picture, proved to be more accurate than the more complicated and detailed theories derived over the next 40 years.

The final pair of contrasting effects caused by collisions concerns heat transport. These can be understood by arguments similar to those just presented for particle transport and thus will not be repeated.

In addition, there is another very important effect of collisions on energy content, the extraction of energy from electric fields. If a DC electric field is applied to a plasma, the electrons will be accelerated. Without collisions, the electrons would simply be lost to the anode. Collisions allow the randomization of the directed energy into a thermal-type distribution. This is called *ohmic heating*. In a related fashion, when an oscillatory field is applied, though the electrons first gain energy, they lose the same amount of energy when the field reverses, unless a collision occurs first. Then again, their momentum is redirected and heating occurs. One new aspect of the collision process is that as temperatures increase, the ease with which charged particles share energy diminishes because the interaction time, hence energy transfer, is smaller at higher velocities. The rate of energy equilibration is given in practical units in the next section.

Let us now turn to a quantitative summary of these phenomena. First consider a weakly ionized unmagnetized plasma with sufficiently high neutral density that they dominate the ion and electron collisions.

Solving the force equation with the addition of a collision term resulting in momentum loss,  $-nmv\nu_m$ , gives an expression for the particle flux,  $\Gamma_j$ ,

$$\Gamma_j = \mu_j n_j E - D \nabla n_j, \quad (45)$$

where

$$\mu_j = |q|/m_j \nu_m, \quad \text{the mobility of the } j^{\text{th}} \text{ species,}$$

$$D = k_0 T / m_j \nu_m, \quad \text{the diffusivity and}$$

$$\nu_m = \tau_m^{-1}, \quad \text{the collision frequency.}$$

Because the electron mobility (Fig. 20) is so much higher than the ion mobility due to the mass dependence, the electrons would tend to run away from the ions. However, then the electric field generated ensures that the ions are pulled along. The net effect is that the transport is ambipolar, and that the effective diffusion coefficient is the mass-weighted mean of the two,

$$D_{eff} = \frac{\mu_e D_i + \mu_i D_e}{\mu_i + \mu_e} \cong 2D_i, \quad (46)$$

for equal ion and electron temperatures.



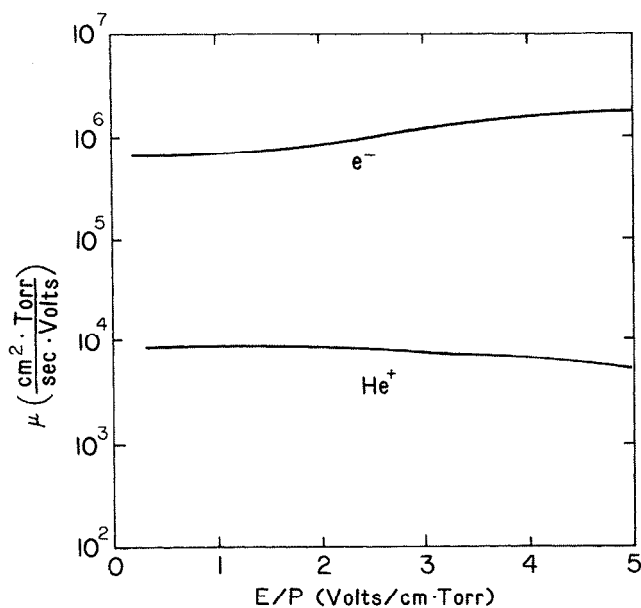


FIGURE 20. Mobilities of electrons and helium ions in helium gas (adapted from Ref. 12).

If the external electric field is shut off, the density distribution will decay in time. The loss processes, being mostly at the wall, ensure that the density there is lowest (Fig. 21). The detailed shape of the density profile depends on where the new plasma is created. The more central the plasma "fueling," the more peaked the density profile.

The inclusion of a magnetic field into this situation requires the inclusion of the  $\mathbf{v} \times \mathbf{B}$  term in the force equation. The result is that the mobilities and

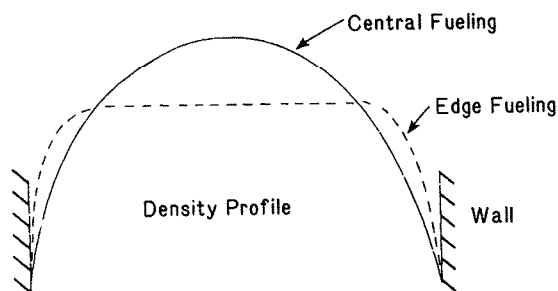


FIGURE 21. Density profile in a plasma device dominated by diffusive losses to the walls. The detailed shape of the profile depends on where the new plasma is created to replenish that which is lost.

diffusivities are modified to

$$\mu_{\perp} = \frac{\mu_i}{1 + \omega_c^2 \tau_m^2} \quad (47)$$

and

$$D_{\perp} = \frac{D}{1 + \omega_c^2 \tau_m^2}. \quad (48)$$

Note the limiting cases for  $D_{\perp}$  show the expected dependence on  $v_m$ .

$$D_{\perp} = \frac{k_B T v_m}{m \omega_c^2} = r_L^2 v_m \quad \text{for } \omega_c^2 \tau_m^2 \gg 1 \quad (49)$$

and

$$D_{\perp} = \frac{k_B T}{m v_m} = \lambda_m^2 v_m \quad \text{for } \omega_c^2 \tau_m^2 \ll 1. \quad (50)$$

For this situation, i.e.,  $B > 0$  and neutral-dominated collisions, particles will diffuse parallel to the gradients and also flow perpendicular to them (and to  $B$ ) at the  $v_D$  and  $v_E$  drift speeds, which are reduced somewhat by neutral-particle drag.

To evaluate the effects of collisions in fully ionized plasmas, we must know the energy-dependent cross section or collision frequency for Coulomb scattering between electrons and ions. An alternate, but equivalent, parameter is the resistivity,  $\eta_{\parallel}$ . This is related to the collision frequency by

$$\eta_{\parallel} = \frac{m_e v_{ei}}{n q^2}, \quad (51)$$

and is equal to

$$\eta_{\parallel} = \pi q^2 m^{1/2} \frac{\ln \Lambda}{(k_B T_e)^{3/2}} \text{ ohm-cm.} \quad (52)$$

The resistivity is the impedance presented by an unmagnetized plasma to a flow of current driven by a static electric field. Note that  $\eta_{\parallel}$  is independent of density. This is because, though the number of charge carriers increases with density, so does the number of scattering centers. The effects exactly cancel.

The term  $\ln \Lambda$  is due to Spitzer, who showed that the correct way to perform the integration over impact distances was to stop at a separation equal to the Debye length at large distances and at the classical radius of the electron at short distances. The value of  $\ln \Lambda$  is about 10 for most laboratory plasmas, ranging from the cold and tenuous glow discharge to hot and dense pinches.

The temperature dependence of  $\eta_{\parallel}$  reflects the fact that as a charged particle's velocity increases, it spends less time near enough to another

charged particle for its trajectory to be greatly altered. So the hotter a plasma, the less effective is ohmic heating.

When a magnetic field is applied, the resistivity parallel to  $B$  is the same, but that perpendicular to  $B$  increases.  $\eta_{\perp}$ , as defined by the collision rate (c.f. Eqn. (51)), is about  $3.3 \eta_{\parallel}$ . But the perpendicular resistivity, as defined by a flow of current in response to an applied electric field, increases much more, about  $3.3(1 + \omega_c^2 \tau_{ei}^2)$ . Remember, in the absence of collisions (e-i, i-i, or quasi-), the application of an electric field to a magnetized plasma results in a drift perpendicular to  $E$  and  $B$ , not current parallel to  $E$ .

Solving for the diffusion of particles, not a flow of current, in this case gives

$$D_{\perp} = \frac{3.3\eta_{\parallel}nkT}{B^2}. \quad (53)$$

In contrast to diffusion caused by neutral impacts,  $D_{\perp}$  depends on the plasma density. So the higher the density, the more rapid the loss. Also note the dependence on  $k_B T_e / B^2$ . This is just the step size,  $r_L^2$ , of the random walk induced by the Coulomb collisions.

The diffusion coefficient in Eqn. (53), however, only represents a lower limit on how quickly plasma will be lost. Experiments usually show a loss rate  $10^4$  times faster. One explanation of this was that presented by Bohm. He estimated that the transport could be driven by self-generated electric field fluctuations in the plasma of strength  $k_B T_e / R$ , where  $R$  is a characteristic distance in the plasma. These would then cause a drift velocity that can be converted into an effective diffusion coefficient

$$D_B = \frac{k_B T_e}{16qB}. \quad (54)$$

The coefficient,  $1/16$ , does not come from Bohm's theory, but is a factor that fits many experiments.

We have seen that there are five different diffusion coefficients (Fig. 22), which may be used to describe the loss of plasma to the walls and other structures of plasma devices. These are:  $D_{\perp}$  and  $D_{\parallel}$  for ion/neutral collisions;  $D_{\perp}$  and  $D_{\parallel}$  for ion/electron collisions; and  $D_B$ . Which is the correct one for a particular situation will depend on the detailed plasma parameters. These will be presented in practical units in the next section. But as rules of thumb, the following guidelines can be used:

1. If the magnetic field is zero and the pressure exceeds  $10^{-2}$  Torr, then the neutral particle collisions dominate plasma transport and resistivity.
2. If the neutral pressure is less than  $10^{-3}$  Torr and a magnetic field  $> 100$  g is present, use  $D_B$  for perpendicular transport of ions and  $2D_{\parallel i}$  for parallel transport.

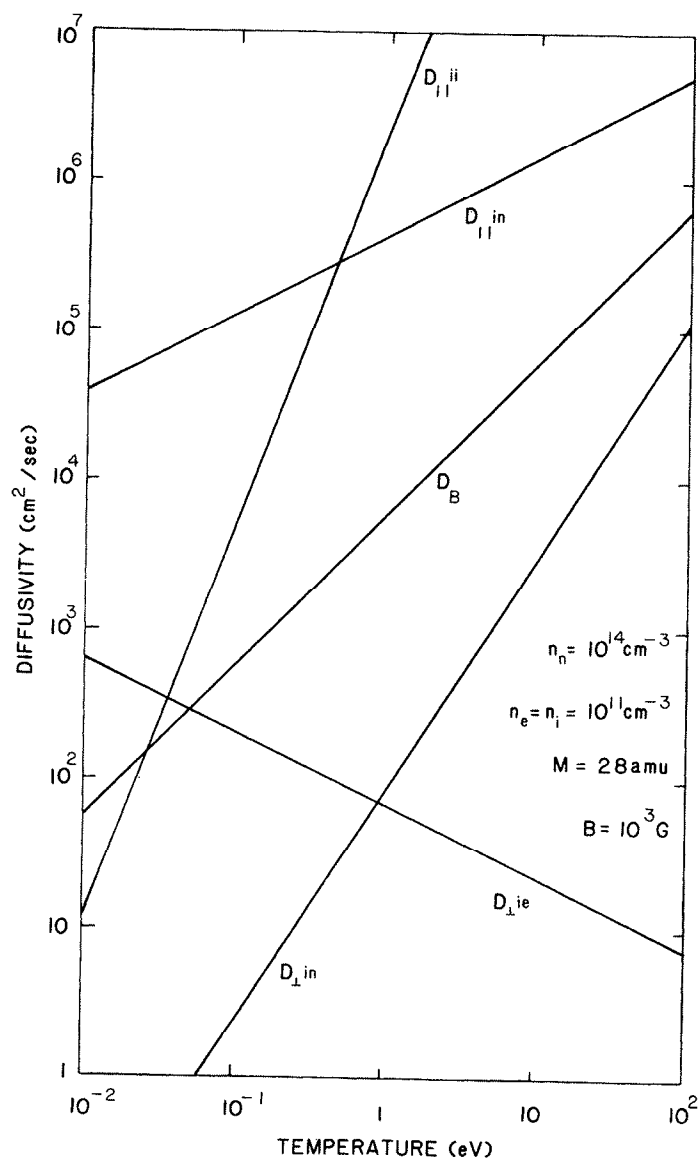


FIGURE 22. Calculated diffusivities as a function of temperature for fixed neutral and electron densities, ion species, and magnetic field.

Collisions of plasma particles with surfaces can be divided into three types depending on the impacting species: neutrals, ions, and electrons. Here we consider only the physical, not chemical, processes. The latter are more appropriately handled in the other chapters of this book.

Neutral atoms and molecules that hit surfaces generally accommodate thermally with the surface and then desorb. Their residence time is typically  $10^{-13}$  sec. This can be altered by cooling the surface or increasing its chemical affinity for the gas atoms. In plasma processing equipment, most neutral atoms have energies of only 1/40 eV. Hence they do not sputter or cause the emission of secondary electrons or ions. A counter-example to this guideline is charge-exchange neutrals formed by interactions of cold neutrals with energetic ions. This would predominantly occur in the sheath where the ions are most energetic. Other counter-examples are molecular fragments (Franck-Condon neutrals) and sputtered atoms. Yet another will be noted shortly.

Ions that impact metal surfaces are rapidly neutralized by the free electrons in the metal unless special conditions are present, one example of which is Cs atoms impinging on solid hot W. The Cs desorbs as ions because the work function of W is lower than the ionization potential of Cs.

The impact of ions can result in their immediate reflection, implantation, and/or delayed release. The immediate reflection is a process that has not

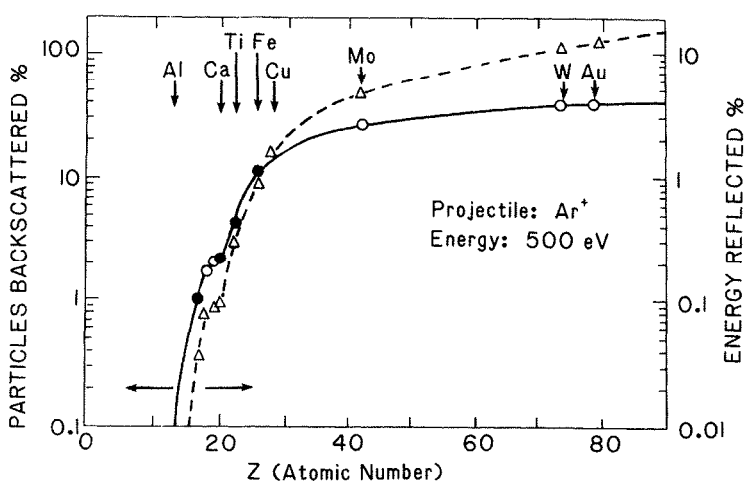


FIGURE 23. Calculated particle and energy reflection coefficients for 500 eV Ar bombardment (normal incidence) of various solids.

tral and

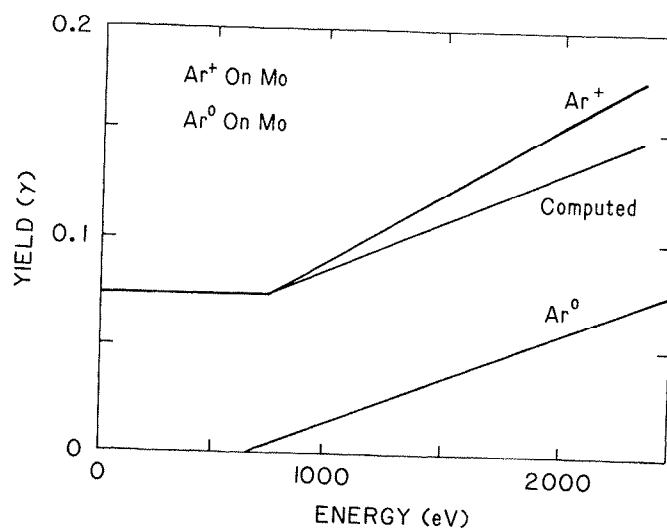


FIGURE 24. Secondary electron yield from molybdenum due to argon atom and ion bombardment (adapted from Ref. 13).

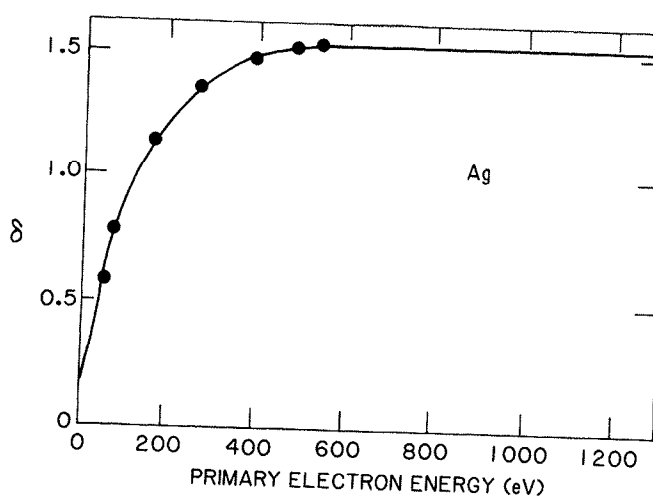


FIGURE 25. Secondary electron emission coefficient from silver as a function of incident electron energy.

been measured accurately. Calculations show the following general behavior (see Fig. 23). If the projectile is more massive than the surface atoms, the projectile will imbed itself in the solid, provided it has enough energy (about 20 eV). If it is less massive, then the projectile will be reflected with about a 30% probability. The reflected atoms have about 30% of their incident energy. The theoretical models are not yet accurate enough to predict the behavior at lower than about 20 eV of energy.

Delayed release is due to diffusion of an implanted atom back to the surface and its subsequent release by thermal desorption, electron-, ion-, or photon-impact desorption, or recombinative desorption.

When ions hit surfaces they can also cause the emission of secondary particles. Sputtered particles are generally of little influence on the plasma behavior; but secondary electrons play a major role. Figure 24 shows the energy-dependent yield of Ar ions and neutrals on Mo. At energies below 1000 eV, potential emission, caused by the deep potential energy well of noble gas ions, gives a constant value for the yield of about 0.1. The yield is about twice larger for He ions and twice lower for Kr ions.

When electrons hit metal surfaces, they too can cause secondaries to be emitted, and their yield can exceed unity. Figure 25 shows the energy-dependent yield for electron bombardment of silver. The yield grows to a maximum at about 400 eV and then slowly decreases.

#### E. SUMMARY OF PLASMA PARAMETERS IN PRACTICAL UNITS

In Table 1 the expressions for the plasma parameters are converted from cgs (electromagnetic) to practical units. In Section III.G. this was done for the drift velocities. We maintain the same definitions here.

#### F. INSTABILITIES

The other phases of matter—gases, liquids, and solids—may be readily prepared in states closely approaching thermodynamic equilibrium. Plasmas, in contrast, rarely exist in the laboratory in such states. In the processes of forming, maintaining, and confining plasmas, numerous nonuniformities and anisotropies develop that can result in instabilities quickly connecting the relatively hot plasma to the cooler walls of the

Table 1

| Parameter                         | Symbol             | Practical Units                               |                          |
|-----------------------------------|--------------------|---|--------------------------|
| density                           | $n$                | $\text{cm}^{-3}$                              |                          |
| ion charge                        | $Z$                | 1 for $H^+$ , 2 for $O^{+2}, \dots$           |                          |
| temperature                       | $T$                | eV  |                          |
| magnetic field                    | $B$                | gauss   |                          |
| ion mass                          | $M$                | amu   |                          |
| Plasma Parameter                  | Symbol             | Expression in Practical Units                 |                          |
| <i>Lengths</i>                    |                    |   |                          |
| electron gyroradius               | $r_{Le}$           | $2.4 T_e^{1/2}/B$                             | cm                       |
| ion gyroradius                    | $r_{Li}$           | $102. (MT_i)^{1/2}/ZB$                        | cm                       |
| Debye length                      | $\lambda_D$        | $743. (T_e/n)^{1/2}$                          | cm                       |
| skin depth (transv)               | $\delta_{\perp}$   | $5.3 \times 10^5 n_e^{-1/2}$                  | cm                       |
| <i>Frequencies</i>                |                    |   |                          |
| plasma frequency                  | $\omega_{pe}$      | $5.64 \times 10^4 n_e^{1/2}$                  | rad/sec                  |
| electron cyclotron                | $\omega_{ce}$      | $1.76 \times 10^7 B$                          | rad/sec                  |
| ion cyclotron                     | $\omega_{ci}$      | $9.58 \times 10^3 B$                          | rad/sec                  |
| collision frequency               |                    |   |                          |
| ion-ion                           | $\nu_{ii}$         | $5. \times 10^{-7} Z^2 n_i / T_i^{3/2}$       | /sec                     |
| electron-electron                 | $\nu_{ee}$         | $3. \times 10^{-5} n_e / T_e^{3/2}$           | /sec                     |
| ion-neutral                       | $\nu_{in}$         | $7. \times 10^{-9} n_n (T_i/M)^{1/2}$         | /sec                     |
| electron-neutral                  | $\nu_{en}$         | $5. \times 10^{-8} n_n T_e^{1/2}$             | /sec                     |
| electron-ion                      |                    |   |                          |
| thermalization<br>( $T_i < T_e$ ) | $\nu_{ei}$         | $3. \times 10^{-9} Z^2 n_e / MT_e^{3/2}$      | /sec                     |
| <i>Diffusivities</i>              |                    |   |                          |
| Bohm                              | $D_B$              | $6.3 \times 10^6 T_e/B$                       | $\text{cm}^2/\text{sec}$ |
| Unmagnetized                      |                    |   |                          |
| ion-neutral                       | $D_{\parallel in}$ | $3. \times 10^{20} (T_i/Mn_n^2)^{1/2}$        | $\text{cm}^2/\text{sec}$ |
| ion-ion                           | $D_{\parallel ii}$ | $4. \times 10^{18} T_i^{5/2}/(Mn_i Z^2)$      | $\text{cm}^2/\text{sec}$ |
| Magnetized                        |                    |   |                          |
| ion-neutral                       | $D_{\perp in}$     | $1.5 \times 10^{-4} n_n (T_i/M)^{3/2}/(ZB)^2$ | $\text{cm}^2/\text{sec}$ |
| ion-electron                      | $D_{\perp ie}$     | $5.5 \times 10^{-4} n_e/(B^2 T_e^{1/2})$      | $\text{cm}^2/\text{sec}$ |
| <i>Miscellaneous</i>              |                    |   |                          |
| plasma parameter                  | $N_D$              | $1.7 \times 10^9 T_e^{3/2}/n_e^{1/2}$         |                          |
| Spitzer resistivity               | $\eta_{\parallel}$ | $0.1 Z/T_e^{3/2}$                             | ohm-cm                   |



containment vessels. In some cases, such as the simple z-pinch, instabilities cause the plasma to disappear rapidly; in other cases, such as the abnormal glow, the plasma may exist in steady state with its instabilities.

In plasmas, the definition of equilibrium is broadened to include any situation that is quasi-static, i.e., where the local parameters do not change with time. This need not be a thermal equilibrium—a Maxwellian distribution need not exist. Instabilities, by this criterion, are processes that tend to bring the plasma to a more uniform spatial or velocity distribution on a time scale faster than the Coulomb-collision time.

What drives instabilities are internally generated electric and magnetic fields. The free energy available to make these fields comes from plasma inhomogeneities, both in density and in velocity space. And if these provide unbalanced forces, individual volume elements of the plasma will be convected toward the walls. The question arises, can plasmas be prepared in configurations where these instabilities do not occur or are unimportant? The answer, from experience, is yes. To understand how this is accomplished, we will review the main categories of instabilities and see what promotes and what stabilizes them.

The usual discussion of instabilities is limited to those that exist in the plasma phase alone, with no regard to plasma-wall type instabilities other than how the wall sets up boundary conditions for the electric and magnetic fields. We shall make an effort to remedy this neglect by including information on unipolar arcs. These are a problem not only for what they do to the plasma (quench it), but also for the stresses they place on the power supplies and for the micron-sized droplets they spray around the interior of the containment vessel.

Instabilities cannot be understood using the single-particle equations of motion alone. In these, there is no feedback mechanism to amplify (or damp) the motion of a particle. So we will rely on a pictorial presentation to clarify the physics concepts. The first step is to set up the classification scheme.

As implied earlier, there are two main sources of free energy that may drive instabilities: nonuniform density and temperature profiles; and non-Maxwellian velocity distributions. The first has the clearly apparent tendency to push plasma from a region of higher temperature, density, or pressure to a region of lower. The second manifests itself by generating waves, which predominantly transport energy from one region to another.

Each of these two major categories is further divided into two: an electrostatic and an electromagnetic subdivision. Electrostatic instabilities result from charge accumulation. If  $B = 0$ , these will usually have a scale size of order  $\lambda_D$ . Electrostatic instabilities along  $B$  will behave similarly.

Electromagnetic instabilities result from and reinforce nonuniform current distributions. Their scale lengths and development times are considerably longer than electrostatic instabilities.

Let us now look at two particular instabilities, one from each of the major divisions. These are chosen because many present-day plasma processing devices should be susceptible to them. Yet the devices work well in spite of or possibly because these are present.

The first is the Rayleigh-Taylor instability. This instability occurs in fluid mechanics when a dense fluid is supported over a light fluid in a gravitational field (Fig. 26). A slight perturbation of the initially flat interface between the two fluids results in the heavier one falling through the lighter; and the lighter one rises. The net effect is a conversion of potential energy into kinetic. If this process is rapid, turbulence may set in, eventually turning the directed kinetic energy into heat.

In plasmas, the situation is rather similar. First we shall describe the closest analog and then generalize to a system more appropriate to plasma processing, a mirror machine.

In the closest analog, a plasma with an inverted density gradient replaces the fluids. And a magnetic field is applied transverse to the gravitational field in an effort to prevent the denser plasma from falling. We start with what should give the best confinement of the plasma by the magnetic field, the ideal MHD (magnetohydrodynamic) assumption. This is that the plasma is such a good electrical conductor any magnetic field that permeates the

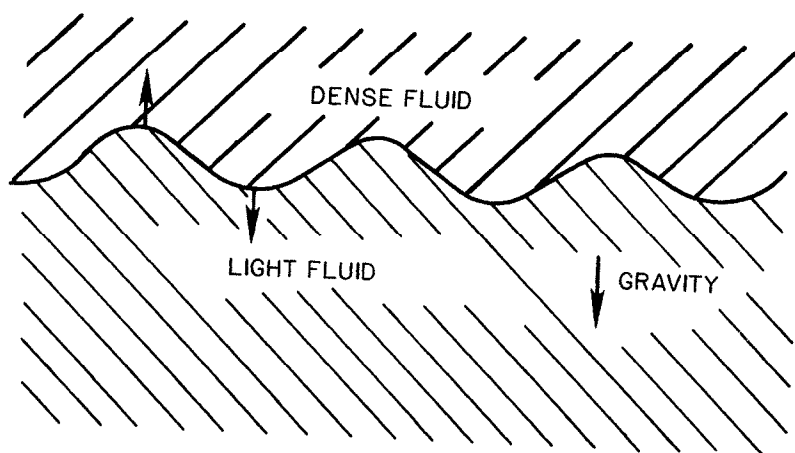


FIGURE 26. Rayleigh-Taylor instability for a dense fluid being supported by a light one in a gravitational field. A perturbation to the fluid interface results in the heavy fluid falling and the light one rising.

plasma is frozen in. In the absence of drift-type motions, charged particles stay on the field lines on which they were born. Will this stop the fall? The picture of what happens when a ripple-shaped perturbation occurs is shown in Fig. 27. The particles of different charge migrate sideways to different sides of the ripples because of the drift due to  $\mathbf{F}_g \times \mathbf{B}$ , i.e.,  $\mathbf{v}_g$ . This sets up an electric field, which then causes a downward  $\mathbf{E} \times \mathbf{B}$  drift of the denser plasma. So the situation is unstable. The magnetic field did not prevent the plasma from falling in the gravitational field.

Of course gravitational forces are unimportant to laboratory plasmas because they are so weak compared to the electric and magnetic ones. So now we go to the mirror machine where a related type of instability, the interchange mode, is predicted and observed to occur.

The gravitational force is replaced by the centrifugal force experienced by the particles as they traverse the curved sections of the magnetic field. When the curvature is outward, as in the central section, we have an exact analogy to the Rayleigh-Taylor problem. The plasma will tend to expand outward there, "falling" into the lower magnetic field region. Nearer to the reflection points, where the  $B$  field is strongest, the curvature, hence the centrifugal force, is inward and the situation is stable. Since particles are constantly moving between the two regions, it is not straightforward to say which region dominates. In the simplest mirror arrangement the situation turns out to be unstable. But judicious shaping of the field by adding other coils can yield stability. The two most common solutions are named Ioffe bars and baseball coils and are shown in Fig. 28. These coils create a region of true minimum  $B$  near the axis of the mirror machine. Then particle excursions away from the axis are accompanied by a restoring force, which prevents the displacement from growing.

The name interchange mode is given to this type of instability because, from the ideal MHD assumption, one sees the picture that as the plasma

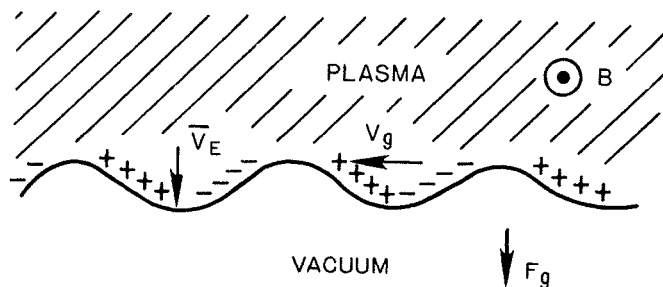


FIGURE 27. Rayleigh-Taylor instability in a magnetized plasma.

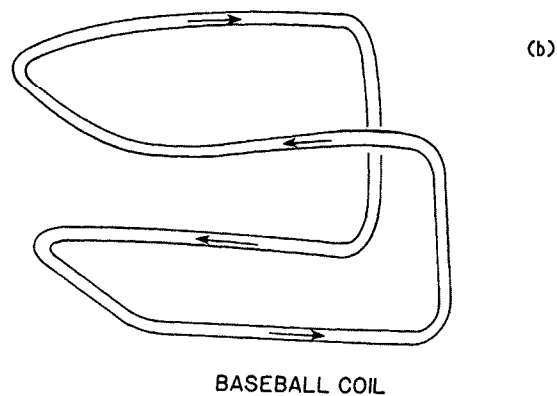
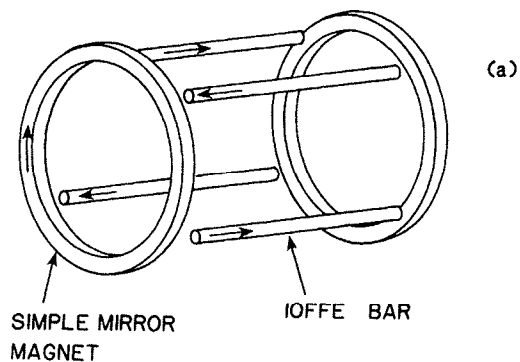
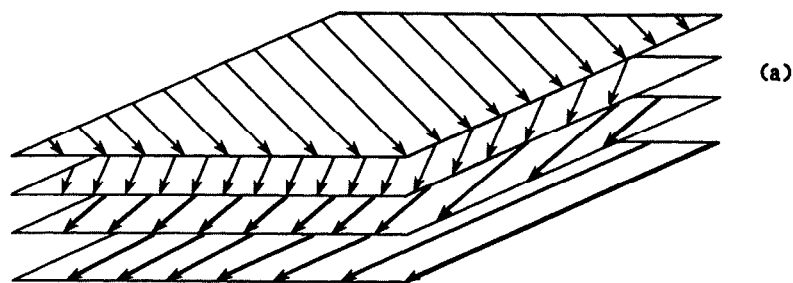
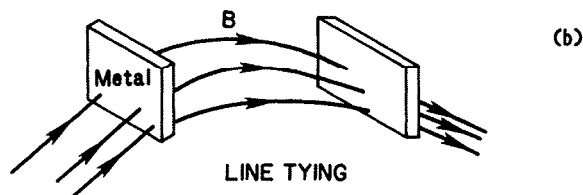


FIGURE 28. a) Stabilization of the simple mirror configuration against Rayleigh-Taylor type instabilities may be obtained by the addition of four Ioffe bars. These cause the net magnetic field to increase with distance from the mirror coil axis. b) Another means to provide stability is to combine the two sets of coils into a single coil with the shape of the stitching on a baseball. The arrows show the direction of current flow.

moves, it carries the magnetic field with it. So, during an instability, one *tube of magnetic flux* may interchange its position with another. This gives yet other views of how to stabilize the plasma. For example, by putting *shear* in the magnetic field (Fig. 29a), one can prevent the flux tubes from sliding past each other. Also by attaching the magnetic field to stationary conductors (Fig. 29b) (remember the plasma is a movable conductor) one



MAGNETIC FIELD WITH SHEAR



LINE TYING

FIGURE 29. Two methods to stabilize interchange modes: a) magnetic shear, and b) line tying.

can inhibit the field from moving. This is called *line-tying*. With the field lines anchored at their ends, the only way plasma motion can carry imbedded field lines is by stretching or bending them. But this frequently requires too much energy. In short, conducting (metal) plates at the ends of the mirrors help to stabilize the plasma.

The instability we just discussed arises from the shape of the confining fields. The configuration caused a spatial deviation from thermodynamic equilibrium. The second type of instability we consider can occur in an infinite and spatially homogeneous plasma. The free energy source is the directed energy of a beam of electrons; the instability is called the two stream. It arises from nonuniformities in velocity space.

In the two-stream instability a beam of particles moves past a counter-streaming beam. Of course one can allow the second beam to be stationary and still get the same results because of translational invariance. For

simplicity, we then consider the second stationary and call it the target. This type of situation occurs in most processing plasmas because secondary electrons liberated from the cathode are accelerated to several hundred electron volts by passing through the cathode sheath. They then move through the relatively cold ( $T \approx 5$  eV) background plasma. Classical Coulomb collisions are too weak to transfer the energy from the beam to the target particles. How then is the energy transferred? By instabilities. Consider a perturbation to the streaming electrons, which, for simplicity in analysis, is a single normal mode of motion for this group of particles. One highly likely mode is the plasma oscillation, but with its frequency now Doppler-shifted by the streaming motion. The phase velocity of the perturbation is then

$$v_p = v_{e0} - \omega_{pe}/k \quad (55)$$

where

$$k = \text{the wave number} = 2\pi/\lambda.$$

When this plasma wave is in resonance with a wave that the target particles can carry, (another normal mode), the wave can grow. This is precisely what happens when the target particles are massive ions. Their plasma frequency is  $(M/m)^{1/2}$  lower than the electrons'. The resonance takes place when

$$v_p = \omega_{pi}/k. \quad (56)$$

Buneman has described this situation with a musical analogy: the ions are the bow and the electrons the string. To be somewhat more precise, one should consider the bow stationary and the violin moving.

The fastest growing modes have frequencies near the plasma frequency. The directed energy of the beam of electrons creates plasma waves with a level much higher than thermal. This then couples to the background electrons and heats them. So in this case an instability has a very beneficial effect. It withdraws energy from the tenuous stream of energetic electrons and heats the denser background of colder electrons.

We now finish our discussion of instabilities with the unipolar arc. As noted earlier, introducing an electrically floating metal object into a plasma results in the build-up of negative charge on the object and a plasma sheath around it. In this analysis we neglected the possibility of electron emission from the metal. Secondary electrons could be emitted due to electron or ion impacts or even photon impacts. These secondary electrons would be accelerated away from the metal by the sheath. A plasma arc may ignite on the metal surface if a small spot overheats due to the emission of secondary electrons. Then the emission process is enhanced by thermionic emission

and the process runs away, i.e., becomes unstable. The arc spot may reemit essentially all the electron current that is collected by the entire metal object. Then the sheath voltage drops and more electron current is collected; and more current may be reemitted through the spot. This is the positive feedback mechanism of the unipolar arc. The cathode is the single solid electrode. The plasma acts as both the other electrode and the electrolyte of this battery (Fig. 30).

When such an arc occurs, the metal object is melted at the arc spot. The metal is explosively released as both vapor and molten droplets of 1 micron typical size. The arc spot on the metal is a few microns in diameter. It is held this small by the combined effects of current channel constriction and thermionic emission. If a magnetic field is present, the arc spot is driven across the surface of the metal by  $\mathbf{J} \times \mathbf{B}$  forces. However, the motion is retrograde, that is, in the opposite sense of what is expected from  $\mathbf{J} \times \mathbf{B}$ . Numerous different mechanisms have been proposed to explain this, but none have yet been proven.

How does one prevent such an arc? There are several methods. First, remove arc initiation sites. These are small embedded insulating occlusions

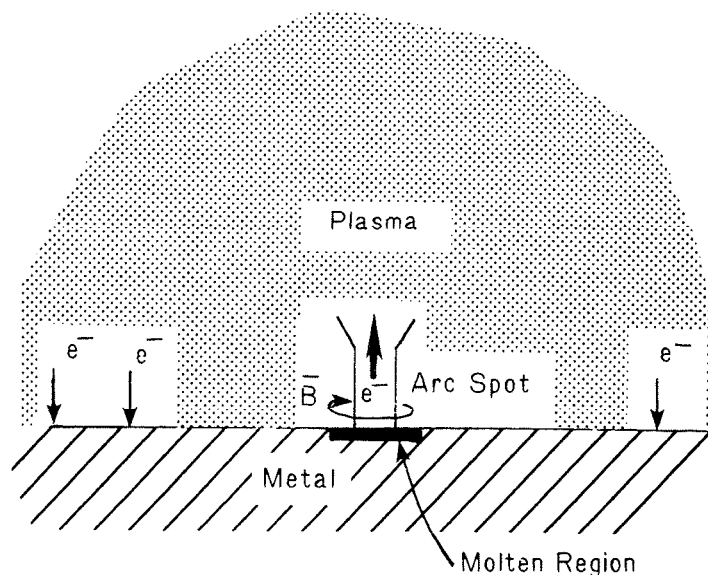


FIGURE 30. Schematic of a unipolar arc. Intense electron emission of all the electrons collected by the entire area of a metal object may occur at one small (1 micron) spot. The metal at that spot melts. The arc will move across the surface of the metal in a direction determined by externally applied magnetic fields interacting with its own fields and currents.

where charge can be built up. Their small size means that strong electric fields will form. Then a spark occurs that ignites the arc. These bits of debris can be removed by standard clean room techniques.

The second method is to avoid metals that form insulating oxides or avoid the formation of oxides. Aluminum is an example of such a problem-prone material. In the case of aluminum, the thin oxide that builds up is a good insulator although it is very thin, 50 Å. Electrons that impact it can raise the potential to a few volts, which then is an electric field of in excess of 10 million volts/cm through the film. The insulating film explodes, releasing many secondary electrons (the Malter effect) and the arc ignites. If aluminum must be used, however, oxygen should be avoided in the plasma chamber. If that too cannot be avoided, then the plasma bombardment of the aluminum must be kept at such a high rate as to keep the aluminum surface clean of oxide.

The third method is to reduce the size of the metal object. This reduces the amount of current that can be reemitted through a potential arc spot.

The final method is to keep the electron temperature low at the metal object. This too reduces the amount of current available to maintain an arc.

## G. PLASMA WAVES

The previous section dealt with instabilities. These can be viewed as over-developed waves. Both start out as normal modes of the plasma motion. But instabilities grow to a point wherein they terminate the plasma or, at least, alter its properties greatly. Waves do not change the plasma much. But exactly how much is the reason for their importance to plasma processing equipment.

The most important application of plasma waves is the heating of plasmas. There are other ways to heat plasmas, ways that do not rely on the resonances implicit in wave heating. One method is classical collisional (Ohmic) heating. This was described earlier. Another method, non-resonant rf heating, will be described in Section V and is also a form of Ohmic heating. There are other applications of waves, such as plasma diagnosis, an old and venerable occupation. These are discussed in another chapter. In this section we review some concepts of wave propagation, list the main types of waves in plasmas, and note which ones will be important for heating process plasmas to increase their temperature and possibly their density.

Before embarking on a discussion of the types of waves that may exist in plasmas, we review some elements of general wave terminology. All the waves we consider are small amplitude; they do not perturb the plasma



greatly. Linearized equations can then be used to see the changes in plasma properties due to the presence of the waves. The waves are also monochromatic; they are describable by a function  $\exp(i(kx - \omega t))$ .

The phase velocity of a wave is given by  $\omega/k$  and the group velocity is given by  $d\omega/dk$ . If all frequencies (or wavelengths) of a particular type of wave have the same phase velocity, the wave is called dispersionless. A wavepacket composed of a group of such waves will propagate without changing shape.

The equation relating  $\omega$  to  $k$  is called the dispersion relation. In solving the dispersion relation for  $\omega$  or  $k$ , complex values may arise. The real parts of the solution correspond to stationary or propagating waves. The imaginary parts correspond to growing or decaying waves; these result from dissipative processes or resonances in the plasma.

Different types of microscopic mechanisms can result in wave growth or decay. Classical collisions with ions, electrons, or neutrals will cause the decay of a wave. Resonances with other waves, as we saw in our discussion of the two-stream instability, can result in wave growth (or decay). *Landau damping* and *inverse-Landau damping* refer to a related phenomenon wherein fast moving electrons "surf" on the crests or in the valleys of charge density (plasma oscillation) waves. In this manner the charged particles either extract energy from or deposit energy into the waves.

As waves propagate through inhomogeneous media, the wavelength will change in a fashion prescribed by the dispersion relation. If the wavelength grows to infinity, a condition called *cutoff*, the wave is reflected. If the wavelength shrinks to zero, a resonance, absorption, occurs.

Coupling a particular wave to a plasma may be a difficult matter. Electrostatic waves do not propagate in vacuum. Hence any antennae or launchers for these must be located in close proximity to the plasma. And as indicated in the previous paragraph, once a wave is launched into a plasma it need not be absorbed. It can be reflected from the plasma interior or be coupled out of the plasma by an electrode in contact with the plasma.

As in the case of instabilities, the understanding of waves can be greatly simplified by categorizing the various modes. This time electrostatic (longitudinal) and electromagnetic (transverse) form the main categories. The next division is usually made based on the species whose properties dominate the wave motion. That is, the subdivisions are electron and ion waves. Ion waves are lower frequency than electron waves because of the greater mass of the ion. Hybrid waves also occur where the coupled motions of both species must be considered in detail.

A further subdivision is based on the role of the magnetic field. If the wave drives the charged particles across  $B$ , cyclotron frequencies naturally occur in the dispersion relation. If the charged particles only have to move

along  $B$  in response to the wave fields, then the wave is usually the same as in an unmagnetized plasma.

Yet another subdivision is based on whether the plasma is hot or cold. This is a loaded question for processing plasmas, which are relatively cool compared to most other plasmas. One tricky aspect of this question is whether gyroradii are large. Then the massive ions, though rather cold, do dominate the thermally modified behavior of certain waves.

With this basic description of waves, we can now state which subdivisions will be of most use in heating process plasmas. First, it is clear that we want to heat electrons in order that the ionization rate increase. Heating ions would be beneficial if it were desirable to have their energies exceed the electrons' energies. However, the sheath is usually adequate for providing ion energy, mostly to ions impacting surfaces. So we will simply ignore ion waves (such as sound waves or ion-cyclotron waves).

To proceed further we must know whether a magnetic field will be present in the particular device. If the answer is no, then there are only two choices, one from each major category. The electrostatic wave turns out to be our old friend the plasma oscillation; only now it has a thermal part in the dispersion relation. The electromagnetic wave is just a standard light wave. In fact, we derived the dispersion relations for these two waves when we were discussing the skin depth (see Eqns. (23) to (37)). It is difficult to heat the plasma interior with a low-frequency electrostatic wave because its plasma skin depth is only the Debye length. But it is not too difficult to get the low-frequency electromagnetic wave to penetrate deep into the plasma. The question is: will it be absorbed? If so, good. If not immediately, then the wave will rattle around inside the metal containment vessel until it is either absorbed by the walls or plasma or can escape through glass (insulating) windows (or feedthroughs). The exact details have to be worked out for each plasma, taking into account resistivity, collisions, the size of the containment vessel (which determines the lowest frequency, or longest wavelength, allowed), and so forth. But this wave is a good candidate for heating plasmas.

If there is a magnetic field present, there are many other types of waves possible. Of course the electron plasma wave could still be used if the  $E$  vector was oriented along  $B$ . Electron cyclotron waves offer an alternative. There are actually three types of electron cyclotron waves, the extraordinary  $X$ , the  $L$ , and the  $R$ . The  $X$  propagates perpendicular to  $B$ ; the  $L$  and  $R$  parallel. In these cases the frequency of the wave is fixed. For a 1000 g field the required frequency,  $\omega/2\pi$ , is about 3 GHz. The wave could be launched from a waveguide a distance from the plasma, but wave absorption would only take place in a narrow region, the resonance zone. Depending on field uniformity, this could range from a few millimeters in size to several centimeters.

## V. Discharge Initiation

Plasma production and maintenance are two processes bound together by the same basic phenomena: ionization and recombination, plasma transport, and plasma-surface interactions; and one inexorably leads into the others. In this section we will discuss two different techniques for initiating plasmas (dc and rf) and describe the processes responsible for determining the electron temperature achieved in one of them during steady-state operation. In both cases we shall see that the electrical parameters present during discharge initiation are rather different from those of the steady-state phase.

### A. DC GLOW

Consider an evacuated glass tube with two internal metal plates separated by a distance  $d$  (Fig. 31) and biased by an external dc power supply. The electric field between the two plates is approximately uniform, except for the fringing field near the plate edges. If a low pressure gas is introduced into the chamber what might occur? A charged particle, say an electron, may be liberated near the negatively biased electrode, the cathode. The cause of this electron could be the passage of a cosmic ray through the apparatus, the decay of a radionuclide in the metal, photo-electron emission by the sun or fluorescent lights, field emission from the metal plate, or a

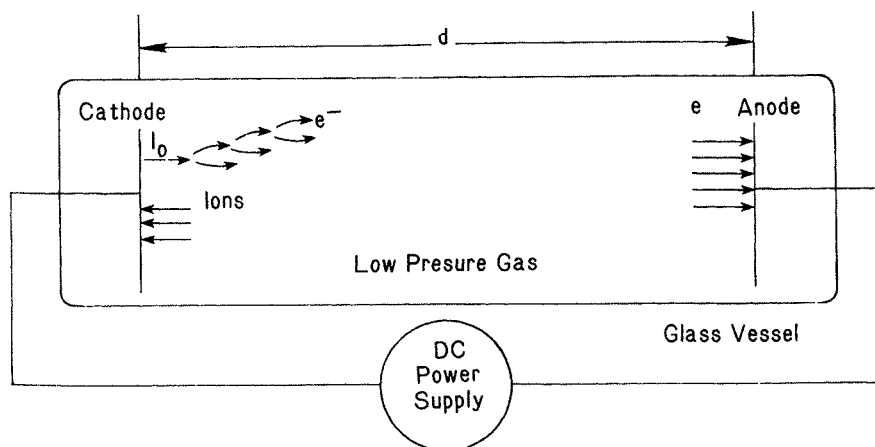


FIGURE 31. Initiation of a glow discharge. An initial current from the cathode is amplified by ionization processes in the low pressure gas. The electrons are collected by the anode. Ions formed in the ionization events are accelerated into the cathode where their impact releases secondary electrons (not shown), restarting the cycle.

host of other processes. The electron now finds itself in the applied electric field and starts to accelerate toward the anode. If the gas pressure is low enough the electron will not suffer any collisions as it proceeds to the anode. It will arrive at the anode, possibly ejecting a secondary electron. However this electron, being born so close to the anode, will simply return there; and there will be no free charges left in our apparatus.

But if the pressure is sufficiently high, the electron will collide with neutral atoms along its path. If the applied electric field is low, the electron will not gain sufficient energy to ionize the atoms. It will simply drift at a speed determined by its mobility. And if the neutral gas is sufficiently electronegative, the electron will attach itself to the atoms. These negative ions will have a substantially smaller mobility.

Let us now consider an applied electric field of such strength that the electron gains enough energy between collisions that it may ionize the next atom it impacts. What happens to the charge pairs created in the volume? The ions drift to the cathode and the electrons to the anode. Secondary electrons are emitted at both. But, as previously noted, only those released from the cathode are useful. The current of electrons toward the anode,  $I_e(x)$ , grows exponentially with distance from the cathode at a rate determined by the number of ionizations per unit distance,  $\alpha$ , the first Townsend coefficient.

$$I_e(x) = (I_0 + \gamma I_i(0)) \exp(\alpha x), \quad (57)$$

where

- $I_0$  = the current of electrons from the cathode due to photo-emission, for example,
- $I_i(0)$  = the current of positive ions onto the cathode, and
- $\gamma$  = the ion impact secondary electron emission coefficient.

The current of ions onto the cathode equals only the ions born in the volume. No ions are born during the creation of the photo-current or the secondary electrons from ion impact. Hence,

$$I_i(0) = I_e(d) - I_0 - \gamma I_i(0). \quad (58)$$

Evaluating Eqn. (57) at  $x = d$  and substituting in Eqn. (58) for the ion current to the cathode gives

$$I_e(d) = \frac{I_0 \exp(\alpha d)}{\{1 - \gamma(\exp(\alpha d) - 1)\}}. \quad (59)$$

Two cases for Eqn. (59) can be readily seen, based on the value of the denominator: i) For small values of  $\alpha$ ,  $\gamma$ , and  $d$ , the denominator is unity so the only current that flows is that released from the cathode by the photons, but amplified slightly by the small value of  $\exp(\alpha d)$ ; ii) For moderate or large values of  $\alpha$ ,  $\gamma$ , and  $d$  (such that the denominator

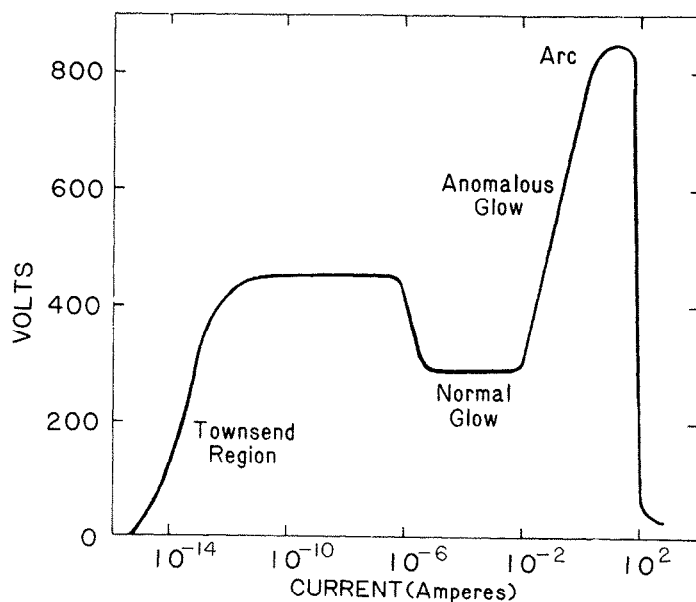


FIGURE 32. Schematic of the I-V characteristics of the apparatus shown in Fig. 31. The metal electrodes are about  $100 \text{ cm}^2$  in area and separated by 30 cm. The gas was air at a pressure of 1 T.

precisely equals zero or is negative) the current grows, faster than exponentially, and breakdown occurs. At this point the equation fails because it does not take into account the decrease of neutral atoms in the system because of ionization or the change of potential in the system, and so forth.

The current that flows in such an apparatus is shown versus voltage in Fig. 32. At low voltages, the current grows with the voltage until the ionization probability, related to  $\alpha$ , approaches a value large enough to break down the gas. Then the Townsend region occurs, and the voltage is constant as the current rapidly rises.

When the gas is highly ionized, i.e., it is a plasma, the electric field between the two plates has been drastically altered. A sheath exists at the cathode, still promoting the acceleration of ions to the cathode and of secondary electrons into the plasma. The glow does not cover all the cathode. An effort to increase the voltage increases the glowing area and the current. This is termed the normal glow. Note that the voltage required to maintain the normal glow is less than that required to achieve breakdown. This type of constant voltage behavior is useful for high-power voltage regulation applications.

Finally, when the entire cathode is covered with a glow, the I-V characteristics change (see Fig. 32), the current does increase with the voltage, and

the abnormal glow has been obtained. This type of discharge is used for many etching processes.

There are several distinct regions of the cathode sheath in a glow discharge. Attached to the cathode itself is the space-charge limited cathode fall region. The ions extracted from the plasma by the cathode fall are limited in current by electrostatic repulsion because the electron density there is less than the ion density. The law describing this was derived by Langmuir and Child for plane parallel geometry and is

$$J_s \text{ (A/cm}^2\text{)} = \frac{5.5 \times 10^{-6} V_s^{3/2}}{M^{1/2} d^2}, \quad (60)$$

with  $V_s$  in volts,  $d$  in cm, and  $M$  in amu. Obviously, from the  $V_s^{3/2}$  and  $d^{-2}$  dependences, the maximum current that can be drawn increases with the electric field. The  $M^{-1/2}$  dependence shows how the particle affects the space charge density near the emitting surface. (For electron emission  $M = 1/1836$ .) From the current drawn and the value of the cathode fall voltage, the thickness of the region can be calculated. The cathode fall represents the largest potential drop in the plasma. Because ions fall through this drop, they extract most, about 80%, of the energy output from the power supply. The secondary electrons emitted from the cathode extract about 20%, the value of the secondary emission coefficient.

Beyond the cathode fall is the Debye sheath (Fig. 33). Its thickness is about five Debye lengths. This is followed by a presheath region [10]. It is

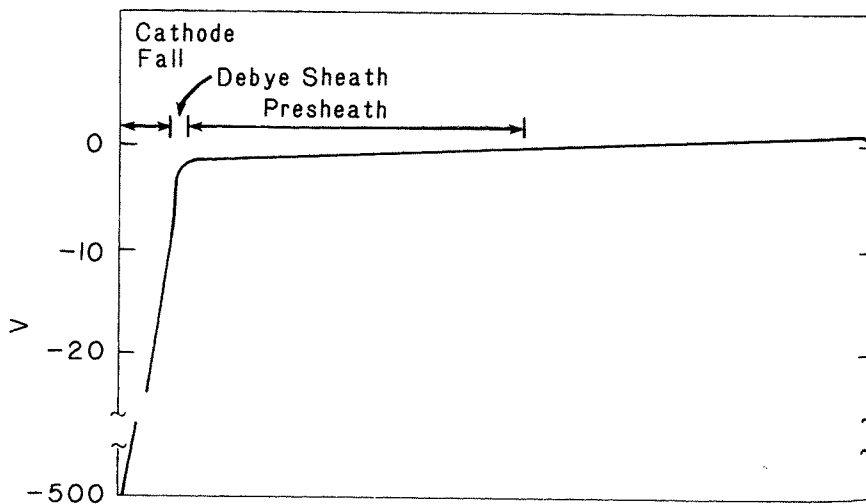


FIGURE 33. Potential as a function of distance for a dc glow discharge.

here that the ions originate which supply the current to the cathode. The continuity condition, called the *Bohm criterion*, relating the flux of ions to the cathode to that from the presheath, requires that the ions leaving the presheath and entering the Debye sheath must have a certain velocity, the ion sound speed. To obtain this velocity, a potential drop of  $0.5T_e$  must exist in the presheath. The thickness of the presheath, defined as the distance this potential drop penetrates, depends on the transport mechanism bringing ions into the presheath. The faster the diffusive flow into the presheath from the bulk plasma, the shorter is the presheath. In Section VI we discuss the effects of magnetic fields on the sheath and justify, by a calculation of ionization rates, where the plasma ions are created. Sheaths, for rf and dc situations, are also discussed in the Langmuir probe section of the chapter on diagnostics.

We conclude this section by noting that there is an optimum (minimum) pressure, for a fixed plate separation, to achieve breakdown. If the pressure exceeds this value, electrons gain less energy before a collision and the ionization probability decreases. If the pressure drops below the optimum, then the electrons travel too far before having an ionizing collision and again the voltage required to breakdown increases. A graph of this behavior, called the Paschen relation, is shown in Fig. 34.

## B. MICROWAVE BREAKDOWN

If a time-varying electric field were applied to the electrodes, little change in breakdown behavior would be noted until the field reversals occurred

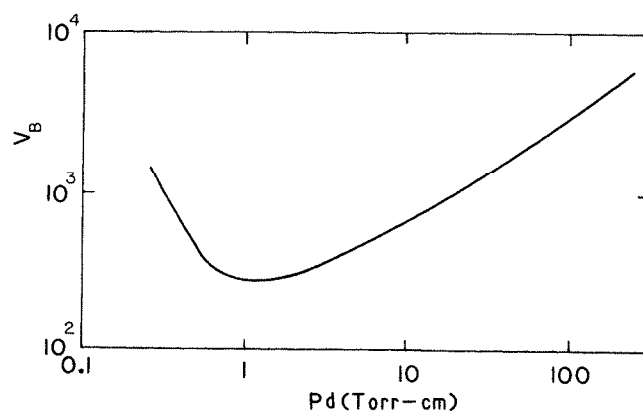


FIGURE 34. Paschen curve, dc breakdown voltage versus pressure  $\times$  plate separation, for hydrogen.

rapidly compared to the particle motions. The slowest particles are the ions. It takes them a few microseconds to traverse the apparatus. Hence, it is not until frequencies of nearly a MHz that an effect is observed. And then it is detrimental; the breakdown voltage rises. The reason is that the rf field interferes with the flow of ions to the cathode, hence fewer secondary electrons are emitted. Once a high enough frequency, about 100 MHz, is applied that the electron losses to the anode via electric-field driven mobility are stemmed, the situation reverses, and a lower breakdown voltage is obtained. At this point the only loss of electrons is by diffusion; and the only loss of electron energy is by collisional heating of the ions and neutrals.

At the walls of the apparatus, the electron losses will build up a sheath. But there is no large cathode fall voltage, only a few  $T_e$ . In contrast to the dc glow, it is clear that here most of the applied (rf) electric field energy is used in creating ions, not accelerating them up to high energies. A hybrid apparatus, with rf discharge production and dc electrode bias, is thus a desirable way to separately control plasma density and ion impact energy.

The rf breakdown voltage shows the same general behavior as exhibited by dc discharges, a minimum in the required voltage as a function of pressure. A scale length enters into this problem in the same way that  $d$  did in the dc analysis. The scale length is now the excursion distance of the electrons instead of the size of the container. Paschen curves for rf breakdown are shown in Fig. 35.

The effective scale size can be further lengthened by applying a magnetic field. Then the electrons are confined axially. And if the applied frequency

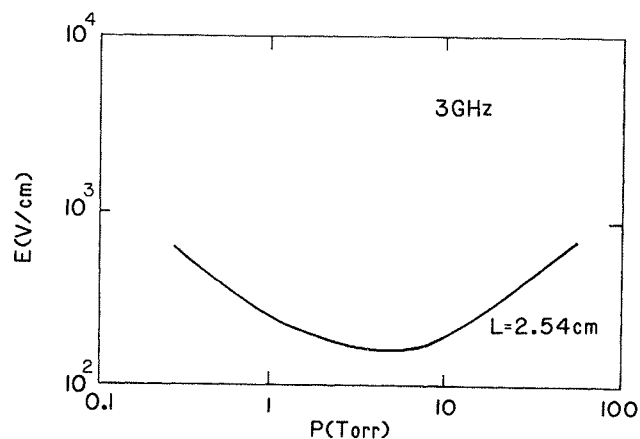


FIGURE 35. Rf Paschen curve for hydrogen in a vessel of 2.54 cm characteristic size (adapted from Ref. 3).



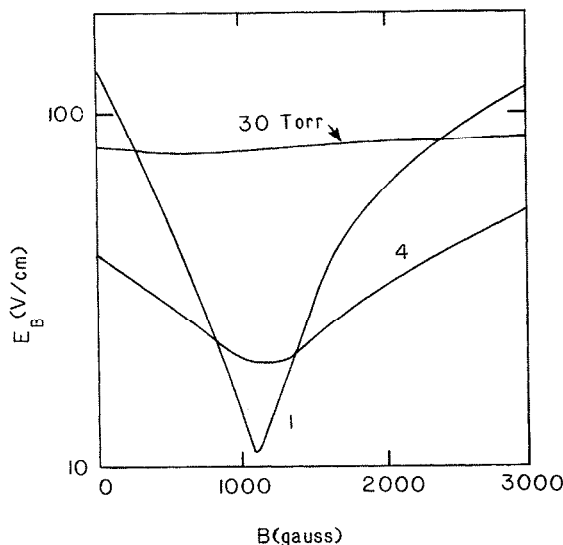


FIGURE 36. The effect of magnetic field on rf breakdown electric field in helium at 3 pressures: 1, 4, and 30 Torr. The applied frequency was 3.1 GHz and the characteristic size was 1.51 cm (adapted from Ref. 3).

matches the electron cyclotron frequency (Fig. 36), then further reduction in required breakdown voltage occurs. This latter improvement is because the electrons now gain energy resonantly from the applied field, instead of “diffusively” as they do when collisional processes are responsible for converting the directed energy into thermal energy.

Let us now examine the electron temperature in a microwave-driven discharge, where the only losses of energy from the electrons are electron-neutral collisions. The force equation is

$$\frac{m dv}{dt} + m\nu_{en}v = -qE_0 \exp(i\omega t), \tag{61}$$

where  $\nu_{en}$  is the collision frequency of electrons with neutrals,  $\omega$  is the frequency of the applied field, and  $E_0$  is its peak amplitude. The solution to this equation is

$$v_f = qE_0 \exp \frac{i\omega t}{i\omega m + m\nu_{en}} \cong \frac{qE\nu_{en}}{m\nu} \tag{62}$$

and the power absorbed by the electrons is

$$P_a = n_n q^2 E_0^2 \frac{\nu_{en}^2}{4m\nu_{en}}, \tag{63}$$

where  $\lambda = v_f/v_{en}$  is the mean free path of the electrons and  $v_f$  is their thermal velocity due to the electric field causing ohmic heating. The loss of energy by the electrons, assumed to be only to the neutrals, is a fraction  $K = 2m/M$  of their thermal energy at each collision. Hence, the energy balance equation is

$$\frac{d \frac{mv_f^2}{2}}{dt} = \frac{qEv_f - Kmv_f^2v_{en}}{2} \quad (64)$$

This can be integrated to yield

$$v_{en}t = \frac{1}{2} \ln \left\{ \frac{1+y}{1-y} \right\} - \tan^{-1} y \quad (65)$$

where  $y = v_f/v_f(t = \infty)$ . Note that

$$v_{en}^{-1} = \left( \frac{1}{2} \right)^{1/4} \left( \frac{m}{e} \right)^2 \left( \frac{1}{K} \right)^{3/4} \left( \frac{\lambda}{E} \right)^{1/2} \quad (66)$$

and

$$v_f(t = \infty) = \left( \frac{2}{K} \right)^{1/4} \left( \frac{e}{m} \right)^{1/2} (E\lambda)^{1/2} \sim \left( \frac{E}{P} \right)^{1/2}. \quad (67)$$

And the energy, proportional to  $v_f^2(t = \infty) \sim E/p$ , is several electron volts. When collisions, or better confinement via magnetic fields, do not form thermal insulation to the wall, it is very difficult to get electron temperatures above  $\approx 5$  eV because the electron thermal conductivity increases proportional to  $T_e^{5/2}$ .

Open geometry parallel plates (Fig. 31) do not work well for coupling power at high frequencies; nor do glass walled vessels retain the transmitted (unabsorbed) rf power. The usual way to form a microwave plasma is inside an all-metal vessel fed by a waveguide.

## VI. An Application—The Planar Magnetron

In the previous sections we discussed single-particle motions, basic plasma behavior, and discharge initiation. Here we apply our newly gained knowledge to understanding how a particular process-plasma configuration works. We choose the planar magnetron because it has a magnetic field, which is mainly parallel to the electrodes. This generally enhances the particle confinement. Configurations with  $B$  normal to the electrodes, as a mirror machine or straight solenoid with end plates, can also get to high plasma densities.

The planar magnetron configuration is more commonly used in deposition than in etching. But related magnetic field shapes have been introduced

into commercial etching equipment. Increases in the size of the planar magnetron make it an attractive configuration for both single wafer and batch-etching applications.

A schematic of a symmetrical magnetron is shown in Fig. 37. This magnetron is a figure of revolution. Also common are ones with a race track shape. The poles face each other across a gap of about 2 to 20 cm. For etching applications the larger gap is appropriate for larger wafers. The field strength at the poles is about 2000 g. The field extends away from the poles in the manner shown in the figure.

The surface to be bombarded (called the target) is placed between the poles. It may be flat (as wafers are), angled, bent, or curved. The surface is biased negatively, either by a dc power supply, or by the rectifying properties of the plasma if rf power (typically at 13.5 MHz) is applied to the surface. If the surface is metallic either method is possible; if it is insulating, only rf can be used.

The magnetron is inside a containment vessel, which is evacuated by a set of pumps, typically including roughing, turbomolecular, and cryogenic. The desired species of gases are bled into the vessel at such a rate that the pressure rises to about  $0.7 \times 10^{-2}$  Torr. For this example let us assume that a mixture of equal parts of  $N_2$  and  $CF_4$  are being used. Again, we will only discuss the physics, not the chemistry, of the discharge. So we are mainly interested in the mass of the ions. For our calculations we assume that all ions are 28 amu. The discharge is initiated by the application of a voltage between the anode ring and the cathode. Once formed, the plasma concentrates near the cathode in a region of relatively high field. The main reason for this shall be seen in the ensuing analysis.

Let us assume that the plasma exists with its known, i.e., measured, properties. Then we will see if it is consistent with our understanding. From Fig. 37 we can read and/or calculate the following magnetron parameters:

|                  |                          |   |
|------------------|--------------------------|---|
| $A$              | = magnetron surface area | = 1000 cm <sup>2</sup> ,                          |
| $V$              | = volume of plasma       | = 1000 cm <sup>3</sup> (brightly glowing volume), |
| $B$              | = average magnetic field | = 1000 g,   |
| $B_M$            | = maximum magnetic field | = 2000 g,   |
| $R_c$            | = field curvature        | = 5 cm,   |
| $\nabla B = B/R$ |                          | = 200 g/cm,                                       |
| $I$              | = magnetron current      | = 10 Amp, and                                     |
| $V_B$            | = cathode bias voltage   | = 500 Volts.                                      |

From the pressure measurements we know

$$n_n = 2.5 \times 10^{14} \text{ cm}^{-3}, \quad \text{and}$$

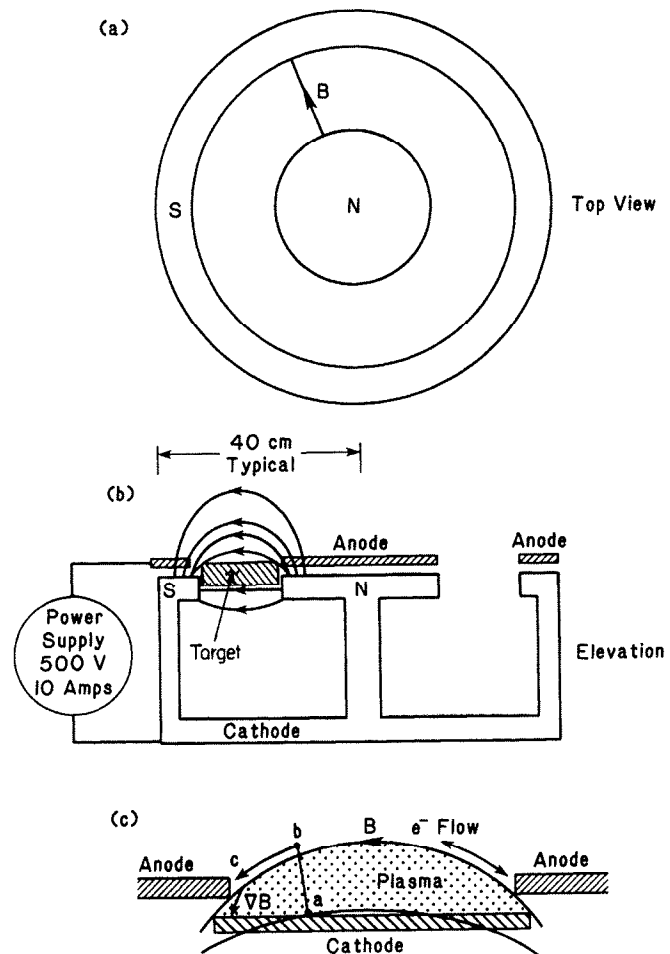


FIGURE 37. Schematic of a circular magnetron. a) Top view showing the magnetic poles. b) Elevation in cross section, showing the placement of the sample surface to be bombarded. The sample may be electrically connected to the poles. Then both would act as the cathode. An anode ring serves to confine the plasma nearer to the sample and away from the containment vessel walls. c) Detail of the sample region showing electron flow along  $B$  to the anode and the direction of the magnetic field gradient at one point. Also shown is the line  $abc$ , which is an axis in Fig. 38.

from Langmuir probes [15] we find

$$T \cong 3 \text{ eV}, \quad \text{and} \\ n_i \cong 2 \times 10^{11} \text{ cm}^{-3}.$$

(Note that these vary with gas pressure, power, and distance from the magnetron.) It is more difficult to get the ion temperature from an experimental measurement. One way is to measure the Doppler shift of radiation. (See Manos and Dylla, Chapter 4.) Let us instead apply our formulae to estimate the ion temperature. The electrons are heated by extracting energy from the electric field. The ions are heated by collisions with the hot electrons. So calculate the ion-electron thermalization time (Section IV.E) getting

$$\nu_{ei}^{-1} = 0.25 \text{ sec.}$$

In contrast, the ion confinement time, found from the ion current to the cathode, is

$$\tau_p = \frac{n_i V}{I \times \text{electrons/coul}} = 3.3 \times 10^{-6} \text{ sec.}$$

We can conclude that the ions in the plasma do not get appreciably heated by collisions with the electrons. They remain near 1/40 eV, room temperature. Of course they will get accelerated in the presheath, in the magnetic sheath, and in the electrostatic sheath.

The first major question we ask is whether the magnetron configuration is stable. From experience, the answer is yes. But what of the Rayleigh-Taylor instability? We predicted that configurations with outward-curving magnetic fields were unstable. We might guess that some stabilizing effects were given by field-line tying to the metallic cathode and anode. Or, more speculatively, we might suggest that the inward electric field balances the outward centrifugal force. But there is actually a clearer reason why no Rayleigh-Taylor instability develops. Let us estimate how long it would take the centrifugal force to move the plasma about  $s = 1/2$  cm. Remember that it is the ions that are most important in this instability. The acceleration,  $a$ , on the massive ions is  $v_{\parallel}^2/R$ . So the time to move 1/2 cm is

$$t = \left( \frac{2s}{a} \right)^{1/2} = 5 \times 10^{-5} \text{ sec,}$$

which is 10 times longer than the lifetime of particles in the plasma. Thus, the plasma ions are lost before the instability can develop. If the confinement were better or the ions more energetic, Rayleigh-Taylor instabilities could well develop.

The next major question to ask is whether the particle densities and temperatures are consistent with the measured current flow (loss,  $L$ , of ions

to the cathode) and the creation rate of ions by electron impact ionization. Start with Eqn. (42) and calculate the predicted rate of ionization. This is multiplied by the electron and neutral densities to get the rate per unit volume. Finally, this is multiplied by the plasma volume to get the total predicted source rate,  $S$ , which can be compared with the ion current

$$S = R_I n_n n_e V = 6.7 \times 10^{19} / \text{sec} \quad \text{versus}$$

$$L = I \times (\text{ions/coul}) = 6 \times 10^{19} / \text{sec.}$$

There is only a 10% discrepancy, which is actually too good. The ionization rate could be in error by 50%; secondary electron emission probably changes the true ion current by 20%; the plasma volume could be off by a factor of 2; and the Langmuir probe data could have 20% errors. Each requires scrutiny in an actual experiment. But we accept the agreement as a sign that we have at least done the zero<sup>th</sup> order atomic physics part of the problem reasonably well. Now use the summary of plasma parameters in Section IV.E to calculate the other basic plasma parameters.

$$\begin{aligned} r_{Le} &= .004 \text{ cm} \\ r_{Li} &= .085 \text{ cm} \quad (1/40) \text{ eV} \\ \lambda_D &= .003 \text{ cm} \\ \delta_{\perp} &= 1.2 \text{ cm} \\ \omega_{pe} &= 2.5 \times 10^{10} \text{ rad/sec} \\ \omega_{ce} &= 1.8 \times 10^{10} \text{ rad/sec} \\ \omega_{ci} &= 9.6 \times 10^6 \text{ rad/sec} \\ \nu_{ii} &= 2.5 \times 10^6 \text{ /sec} \\ \nu_{ce} &= 1.2 \times 10^6 \text{ /sec} \\ \nu_{in} &= 5.2 \times 10^4 \text{ /sec} \\ \nu_{en} &= 2.2 \times 10^7 \text{ /sec} \\ \nu_{ei} &= 4 \text{ /sec} \\ D_B &= 1.9 \times 10^4 \text{ cm}^2/\text{sec} \\ D_{\parallel in} &= 3.6 \times 10^4 \text{ cm}^2/\text{sec} \\ D_{\parallel ii} &= 71 \text{ cm}^2/\text{sec} \\ D_{\perp in} &= 1 \text{ cm}^2/\text{sec} \\ D_{\perp ie} &= 65 \text{ cm}^2/\text{sec} \\ N_D &= 1.9 \times 10^4 \\ \eta_{\parallel} &= .019 \text{ ohm-cm} \end{aligned}$$

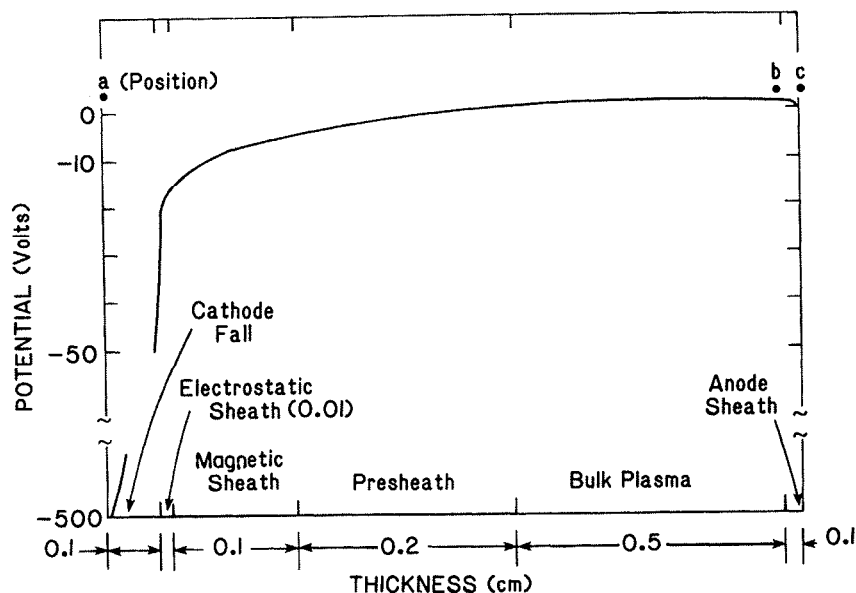


FIGURE 38. Potential along the line abc in Fig. 37. The approximate thicknesses of each region are shown. The potential drop in the anode sheath occurs in the last .01 cm in the  $B$ -perpendicular direction and then all along the arc length bc.

We shall now proceed to calculate the particle trajectories. (For experiments describing related measurements, see Ref. [16].) To do this, the electric and magnetic fields inside the plasma are needed. The magnetic field is predominantly the applied one because the current through the plasma, 10 amps, only causes fields  $< 1$  gauss. In contrast, the electric fields are greatly controlled by the plasma. There are both an electrostatic (e.s.) and a magnetic sheath, as shown in Fig. 38. And also a cathode bias voltage zone is present. The electric field for these different regions is shown also in Fig. 38. The strongest field is in the electrostatic sheath, because it is the thinnest. But the field due to the cathode fall is also large. The field in the magnetic sheath is a few percent of that in the electrostatic sheath. With this and the gradients listed earlier, we can now calculate the drift velocities.

Consider the secondary electrons emitted from the cathode. They enter into an electric field of several thousand V/cm. This quickly accelerates them away from the cathode. This occurs before  $v_{\nabla B}$  or  $v_E$  can develop. So these electrons get up to about 500 eV and pass through the cathode fall and the e.s. sheath into the magnetic sheath. Had we calculated  $v_E$  in the

e.s. sheath and the cathode fall, these would have corresponded to energies in excess of that to be gained from the electric field ( $W = qE \times \text{distance}$ ). These regions are too short to allow the drift approximation to be valid. Once in the magnetic sheath the drift approximation is valid even for these 500 eV electrons. Their Larmor radii are about 1/6 of the thickness of the magnetic sheath.

Most of the energy the electrons gained in passing through the cathode fall region was in the direction perpendicular to  $B$ . So they, of course, are spiraling around  $B$  at their cyclotron frequency. These electrons also move along the magnetic field rapidly, at about  $10^9$  cm/sec. And because of the shape of the magnetic field, they are brought back toward the cathode surface. But most of their energy is, initially at least, perpendicular to  $B$ . Combined with the magnetic mirror effect and energy loss to the plasma (via instabilities, for example) it is highly unlikely that the hot electrons will ever again reach the cathode. And the hot electrons are well confined in the plasma—by electrostatic effects parallel to  $B$  and by the field itself in the perpendicular direction.

In the magnetic sheath, the hot electrons are also executing drift motions due to the electric and curved  $B$  fields. These drift velocities are about  $3 \times 10^7$  cm/sec, a small fraction of their total velocity. These drifts take the electrons on orbits around the magnetron (Fig. 39). The net pattern of their motions is a zig-zag between the inner and outer poles.

The energy loss processes for these hot electrons include ionization, e-e scattering, e-i scattering, and e-n scattering, as well as instabilities. Using the formulae in section IV.D, these can be evaluated. The time it takes a 500 eV electron to ionize (see Fig. 18) an atom is about  $5 \times 10^{-8}$  sec, during which the electron will drift about 1.5 cm perpendicular to  $B$ . In that type of collision the electron loses about 10 eV. Collisions that simply excite the atoms are even more numerous. The net effect is that these electrons lose about 30 eV per cm of drift circuit around the magnetron. And in the process they create a new cold (about 1 eV) electron about every cm.

Coulomb collisions with these cold electrons occur at a  $10^4$  slower rate. And e-i collisions are even less effective at withdrawing the energy from the hot electrons.

No simple formula was given for the energy loss to instabilities. Indeed it is hard to relate, quantitatively, one experiment of this type to another. With that caveat we note that the measured energy loss e-folding distance for a two-stream type instability has been found to be about 10 cm for 500 eV electrons in  $\times 100$  less dense plasmas. But even if that slow rate applied here, then the  $B$ -parallel velocity of the hot electrons, being so large compared to the drift velocity ( $10^9$  vs  $3 \times 10^7$  cm/sec), would result in an energy loss rate of 250 eV per cm of circuit (perpendicular to  $B$ ) around the magnetron.



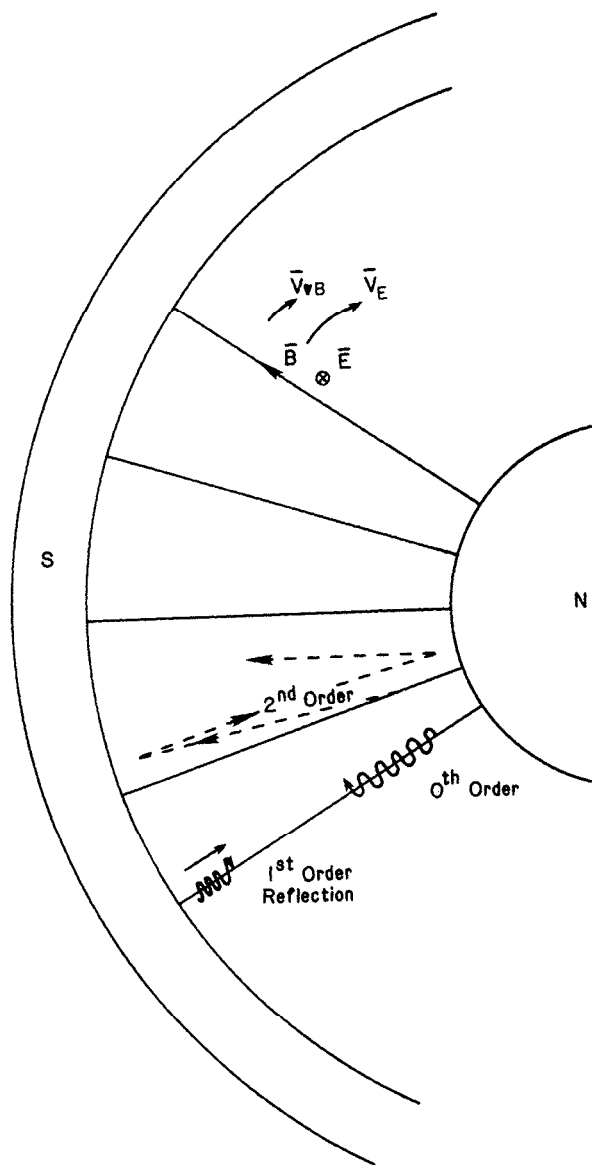


FIGURE 39. Motion of electrons in a magnetron. At 0<sup>th</sup> order, only the cyclotron motion around  $B$  and flow along  $B$  are included. The 1<sup>st</sup> order correction to the motion includes reflection as the electrons enter regions of increasing  $B$  and decreasing potential. The 2<sup>nd</sup> order description includes drift motion due to the crossed  $E$  and  $B$  fields and the grad  $B$  and curved  $B$  (not shown) fields. Plasma instabilities and ionization events prevent hot electrons from circulating around the magnetron without energy loss.

And so we conclude that the hot electrons do not circulate around the magnetron, but dissipate their energy mainly (90%) to warming the cold electrons (via instabilities) and also to creating new electrons (10%). It is interesting to note that for each ion that hits the cathode, about 0.2 secondary electrons are liberated. And for each secondary electron entering the magnetic sheath at 500 eV less than 0.5 direct ionizations occur. So these hot electrons replenish less than 10% of the electrons lost by flow to the anode.

The hot electrons have a density, calculated from the ion current, the secondary electron yield, and the sheath voltage of about  $4 \times 10^7 \text{ cm}^{-3}$  in the cathode fall region, and about the same in the magnetic sheath (but calculated from the energy loss rate and sheath thickness).

From the e.s. sheath region out to the anode exists the bulk plasma whose electrons have a measured temperature of about 3 eV. Previously we saw that they explain the maintenance of the plasma, i.e., their ionization rate balanced the particle loss rate. In the magnetic sheath, these electrons have a  $v_E$  about 10% of their thermal velocity. In the presheath it is 0.1% of  $v_t$ . The grad  $B$  drift is similarly unimportant. The electrons also have a drift parallel to  $E$ , due to their transverse mobility. After traversing about 1 cm perpendicular to the field, they encounter a field line connected to the anode. From there they flow parallel to  $B$ , reach the anode, and complete the electrical circuit, which began at the power supply connection to the cathode. This picture shows why the plasma has little extent away from the cathode.

Does the calculated electron mobility correctly explain the electron flow to the anode? There are two parts to this question: flow parallel to  $B$  and flow perpendicular to  $B$ . Both involve evaluating Eqn. (45) with the mobilities obtained from the diffusivities and the definitions in Eqn. (45). For parallel motion there is no trouble getting agreement. The electrons flow collisionlessly to the anode along  $B$  ( $v_{ei,n} \ll v_t/d$ ). The parallel resistivity gives good agreement if one assumes an anode drop of 3 eV, and dimensions of 10 cm length and 0.1 cm thickness of the  $B$ -parallel region. For perpendicular motion it should come as no surprise to hear that the classical electron-ion  $D = 65 \text{ cm}^2/\text{sec}$ , and  $\mu_2$  are too small by about a factor of 1000. The mobility calculated from Bohm  $D_B$  is too small by about a factor of 3, which isn't bad agreement. The perpendicular resistivity of the plasma, including the collisional correction  $(1 + \omega_{ce}\tau_m)$  also gives agreement to about a factor of 3.

Let us now consider the ion motion, starting from the region where most ions originate, the positive column. There the ion motion is well described by the drift equations, because the Larmor radius (for 1/40 eV) is small compared to the size of the region. The thermal velocity is small,

$4.2 \times 10^4$  cm/sec;  $v_{\nabla B}$  is smaller =  $10^3$  cm/sec; and  $v_E$  is near zero. The ions diffuse into the presheath and are accelerated up to the ion sound speed, about  $3 \times 10^5$  cm/sec, as they are attracted to the cathode. The drift speeds increase because of the increase in  $E$  and  $W$ :  $v_{\nabla B} = 6 \times 10^4$  cm/sec and  $v_E = 3 \times 10^5$  cm/sec. It is here in the presheath that the drift approximation for the ions fails. The ion gyroradii at 3 eV is about 1 cm, equal to the size of the entire plasma thickness.

The ions are further accelerated as they enter the magnetic and e.s. sheaths. Their velocity at the entrance to the e.s. sheath is estimated to be about 3 times the sound speed. The increase above the sound speed is due to the "impedance" magnetic field.

And finally upon reaching the cathode drop, the ions start their final acceleration up to 500 eV. The effects of the magnetic field are small. A detailed calculation should be done to obtain the angle of impact of the ions on the cathode. Based on the fact that the ions can only complete  $\approx .01$  gyroradius during their final acceleration, we estimate that the angle of impact is within a degree of the surface normal.

The flow of the ions is what provides all the current to the cathode. Let us check if it agrees with the measured current. Simply multiply the ion density times the sound speed times the magnetron area,

$$I = (2 \times 10^{11})(3 \times 10^5)(1000)(1.6 \times 10^{-19} \text{ coul/e}) = 10 \text{ amps,}$$

which agrees with the magnetron current. So the most abundant energetic particles are 500 eV ions. They account for about 80% of the power loss. And this goes to the cathode. To reduce the power loss to the cathode, and the possibility of lattice damage there, it would be desirable to maintain the ion current (even to increase it) but reduce the ion energy. This could be done by increasing the plasma density and temperature, both of which increase the mobilities and diffusivities. One way to accomplish this might be electron heating at the electron cyclotron frequency. For this magnetic field, the electron cyclotron frequency is close to that used in microwave ovens.

The reader has now seen that the basic operation of a process plasma device can be understood from the fundamental properties of plasmas. The density and its distribution within the chamber, the temperature and energies of the ions, electrons and neutrals, the currents that flow to the different electrodes—all these can be predicted before building an apparatus. And if changes are required in a particular aspect, then the most likely methods to obtain the desired result can be identified by a careful examination of the fundamental laws.

### Acknowledgements

I thank the JET project, Oxfordshire, England for its hospitality during the time this manuscript was written, and Dr. D. M. Manos, Dr. S. M. Rossnagel, and Prof. P. C. Stangeby for their comments on the manuscript.

### References

- [1] F. Llewellyn-Jones, "The Glow Discharge." Methuen and Co., London (1966).
- [2] J. L. Vossen and W. Kern, editors, "Thin Film Processes." Academic Press, New York (1978).
- [3] A. D. MacDonald, "Microwave Breakdown in Gases." John Wiley and Sons, New York (1966).
- [4] "The Collected Works of Irving Langmuir." Pergamon Press, Oxford (1961).
- [5] J. M. Meek and J. D. Craggs, "Electrical Breakdown of Gases." Clarendon Press, Oxford (1971).
- [6] N. A. Krall and A. W. Trivelpiece, "Principles of Plasma Physics." McGraw-Hill, New York (1973).
- [7] L. Spitzer, "Physics of Fully Ionized Gases." (2nd edition). Interscience, New York (1962).
- [8] F. F. Chen, "Introduction to Plasma Physics." (2nd edition). Plenum Press, New York (1980).
- [9] A. von Engel, "Ionized Gases." Clarendon Press, Oxford (1955).
- [10] D. Post and R. Behrisch, editors, "Physics of Plasma-Wall Interactions in Controlled Fusion." Plenum Press, New York (1984).
- [11] B. Chapman, "Glow Discharge Processes." John Wiley and Sons, New York (1980).
- [12] S. C. Brown, "Introduction to Electrical Discharges in Gases." John Wiley and Sons, New York (1967).
- [13] G. Carter and J. S. Colligon, "Ion Impact of Solids." Heinemann, London (1968).
- [14] J. M. Lafferty, editor, "Vacuum Arcs." John Wiley and Sons, New York (1980).
- [15] S. M. Rossnagel and H. R. Kaufman, Langmuir Probe Characterization of Magnetron Operation. *J. Vac. Sci. and Technol.* A4, 1822 (1986).
- [16] S. M. Rossnagel and H. R. Kaufman, Induced Drift Currents in Circular Magnetrons. *J. Vac. Sci. and Technol.* A5, 88 (1987).